

A new mixed model based on the enhanced-Refined Zigzag Theory for the analysis of thick multilayered composite plates

Original

A new mixed model based on the enhanced-Refined Zigzag Theory for the analysis of thick multilayered composite plates / Sorrenti, M.; Gherlone, M.. - In: COMPOSITE STRUCTURES. - ISSN 0263-8223. - ELETTRONICO. - 311:(2023). [10.1016/j.compstruct.2023.116787]

Availability:

This version is available at: 11583/2976491 since: 2023-11-20T08:30:53Z

Publisher:

Elsevier

Published

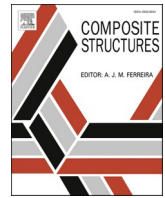
DOI:10.1016/j.compstruct.2023.116787

Terms of use:

This article is made available under terms and conditions as specified in the corresponding bibliographic description in the repository

Publisher copyright

(Article begins on next page)



A new mixed model based on the enhanced-Refined Zigzag Theory for the analysis of thick multilayered composite plates

M. Sorrenti^{*}, M. Gherlone

Department of Mechanical and Aerospace Engineering – Politecnico di Torino, Corso Duca degli Abruzzi 24, 10129 Torino, Italy

ARTICLE INFO

Keywords:

Angle-ply laminates
Sandwich plates
Multilayered plates
Enhanced Refined Zigzag Theory
Hellinger-Reissner functional
Transverse normal deformability
Bending

ABSTRACT

In this paper, a new mixed model based on the enhanced Refined Zigzag Theory for thick multilayered composite plates is formulated. The kinematics is assumed cubic for the in-plane displacements and parabolic for the transverse one. The set of kinematic variables are reduced by using a partial constraint on the transverse shear stress, and a new set of enhanced cubic zigzag functions are obtained. The transverse normal stress is assumed as a smeared cubic function along the laminate thickness. The assumed transverse shear stresses profile is derived from the integration of local three-dimensional equilibrium equations involving a new set of strain variables. The entire formulation is developed by involving the Hellinger-Reissner functional and a penalty term for the strains compatibility; the governing equations and the consistent boundary conditions are derived. Finally, to assess the proposed model's predictive capabilities for general multilayered laminated and sandwich plates, results are compared with exact three-dimensional solutions available in the literature.

1. Introduction

In the recent years, the use of composite materials has widely increased in various engineering fields (aerospace, automotive, marine, military, civil, ...) due to their excellent properties, such as high stiffness-to-weight ratio and good fatigue behaviour under cycle loads. On the other hand, they exhibit high transverse anisotropy and transverse shear deformability that have to be taken into account during the design in order to prevent failures, such as delamination.

Among the numerical models existing in the literature framework, very few works on analytical three-dimensional solutions have been provided. In Pagano's works [1,2], a solution for the cylindrical bending and bending of simply supported multilayered and sandwich plates has been proposed. For more general laminated plates, such as symmetric and unsymmetric angle-ply, Pagano [3] provided a three-dimensional analytical solution under the hypothesis of cylindrical bending and simply-supported edges. Among the exact elasticity solutions for anti-symmetric laminate plates, Noor and Burton [4] have developed a mixed formulation for stress and free vibration problems. Later, Savoia and Reddy [5] have used a variational approach for the three-dimensional static solution of rectangular antisymmetric angle-ply multilayered plates with simply supported edges. Although the exact elasticity solutions are desirable in order to describe the correct behaviour of

multilayered composite and sandwich plates, unfortunately, simply-supported boundary conditions are rarely found in industrial applications. Without involving the use of solid finite element models for complex structures, since they are affected by prohibitive computational costs, it is necessary to develop other structural models to achieve a reliable solution.

In order to pursue this aim, axiomatic displacement-based theories are the most used for structural analysis. They can be grouped into two main categories: the Equivalent Single Layer (ESL) theories and the Layerwise (LW) ones. The displacement field assumed in the ESL theories is independent of the number of layers. Generally, they provide accurate results for global quantities (transverse displacements, natural frequencies and buckling loads), but they are quite inaccurate for the through-the-thickness displacements, strains and stresses. In the LW theories, an independent displacement field is assumed for each layer, with the continuity of displacements at the layer's interfaces.

Moreover, it is also possible to enforce the through-the-thickness transverse shear stresses continuity that cannot be obtained in the ESL theories. Among the most used ESL theories the Classical Laminate Theory (CLT), the First-Order Shear Deformation Theory (FSDT) and the Third-Order Shear Deformation Theory (TSTD) have been widely used. More details on the hypotheses, formulations and numerical examples of these models can be found in the book of Reddy [6]. Although the LW

^{*} Corresponding author.

E-mail addresses: matteo.sorrenti@polito.it (M. Sorrenti), marco.gherlone@polito.it (M. Gherlone).

are more accurate than the ESL ones, the computational cost is not affordable for structures with several layers. The interested reader is referred to the reviews of Di Sciuva and Abrate [7,8] and Li [9] for a more general overview on existing ESL/LW theories.

In recent years, the Zigzag Theories (ZZT) have been widely used as alternative structural models with respect to the ESL and LW theories. Generally, the kinematic field of these models regarding the in-plane displacements is represented by a superposition of a coarse distribution (such as in the ESL assumptions) and a finer one described by zigzag functions. Zigzag models have more kinematic variables than the ESL ones but are computationally efficient with respect to the Layerwise. In the open literature, several ZZTs have been developed that differ from one another for the methodology implemented to derive the zigzag functions. This enhancement in the displacement field leads to a more accurate prediction of through-the-thickness quantities, particularly for the transverse shear stresses. In the past, several researchers have developed zigzag models (Di Sciuva [10,11], Cho and Parmerter [12], Murakami [13] and Icardi [14], that represent the first contributions in this field).

The Refined Zigzag Theory (RZT), originally developed by Tessler et al. [15,16], has been widely used in recent years for the analysis of multilayered and sandwich beams [17–20], plates [21–24] and shells [25–27], revealing to be very accurate for displacements and in-plane stress through-the-thickness distributions. In RZT, the global first-order kinematic, typical of the FSDT, is enriched with continuous piecewise linear zigzag functions, whose slope is a piecewise constant function with jumps at the interfaces. The linear zigzag functions are then derived through a partial fulfilment of the transverse shear stress continuity at the layer interfaces. Moreover, an attractive aspect for efficient finite element implementation is that the RZT requires only a C^0 continuity for the seven kinematic variables.

Recently, the standard zigzag kinematic has been enriched with two additional zigzag functions in order to consider the coupling effect of in-plane displacements typically present in angle-ply stacking sequence. This peculiar behaviour was observed firstly by Whitney [28], more recently, by Di Sciuva [29] using a zigzag model and by Loredo and co-workers [30–33] that developed a new model in which a set of warping shear functions obtained from the three-dimensional elasticity are used to improve the kinematic field. The new set of enhanced zigzag functions, formulated according to the procedure of RZT, does not increase the number of (seven) kinematic variables of the standard RZT. This new model, the enhanced-RZT (en-RZT), has shown [34,35] to generally predict displacements, frequencies and through-the-thickness distributions of stresses in angle-ply laminates.

The transverse shear stress distributions coming from the material constitutive relations in the RZT are not accurately represented, since this theory fails to guarantee the full through-the-thickness stress continuity at the layer interfaces. As a consequence, the transverse shear stresses are more often obtained by the integration of the local equilibrium equations providing highly accurate distributions for the RZT model. Moreover, the exact elasticity solutions have shown that the transverse normal deformability is no more negligible, and the in-plane displacements have a more complex distribution [36] for sandwich laminates, especially if the plate is moderately thick to thick.

In order to include these effects, among the existent works on the RZT, the in-plane kinematics has been enriched by Barut et al. [37,38] by using a quadratic through-the-thickness variation of the in-plane and transverse displacements. In their model, the transverse normal stress is assumed as a continuous cubic function related to an independent field, then a least-square statement is used to enforce the transverse normal strain compatibility. In a similar way, Iurlaro et al. [39–42] have enriched the RZT in-plane kinematics with a smeared parabolic contribution and layerwise cubic terms in the thickness coordinate, whereas, for the transverse displacement, a smeared parabolic distribution has been assumed, which depends on the top, bottom and average transverse displacements. The number of kinematic variables is reduced by

enforcing the top/bottom transverse shear stress-free conditions, resulting in an in-plane kinematic field with piecewise cubic zigzag functions. In this model, called RZT_(3,2)^(m), the transverse normal stress is assumed as an independent field, with a smeared cubic distribution that satisfies the equilibrium stress conditions on the outer surfaces. According to the assumption proposed by Tessler [43], the transverse shear stresses have been assumed as independent fields where the through-the-thickness the transverse distributions are obtained directly by integrating the local three-dimensional equilibrium equations under the hypothesis of cylindrical bending. The Reissner's Mixed Variational Theorem (RMVT) [44] is then used to relate the independent stress variables to the kinematic ones. Although this procedure has been demonstrated to provide accurate results for multilayered composite and sandwich plates [42], the cylindrical bending hypothesis is a strong reduction and simplification of the plate behaviour, especially for angle-ply laminates. This assumption developed to avoid over-fitting transverse shear stress distributions (as shown by Auricchio and Sacco [45] for the FSDT) is no longer valid when more general stacking sequences are considered, i.e. angle-ply.

In a similar way, Groh and Weaver [46] have used the linear RZT with a third order expansion of the in-plane displacements in conjunction with the use of the Hellinger-Reissner (HR) mixed variational theorem to investigate the static behaviour of highly heterogeneous laminated beams. It has shown that the HR formulation was able to capture the transverse stresses very accurately (over-performing the RMVT) without involving any post-processing procedure. The previous two field mixed formulation has been extended by the same authors to investigate the three-dimensional static behaviour of heterogeneous laminated plates [47,48]. The same theory has been used by Thurnherr et al. [49] to accurately predict the stresses in curved multilayered beams. Köppl and Wagner [50] have formulated a quadrilateral plate element involving the RZT kinematic and a modified HR functional where the displacements and the transverse shear stresses are involved as independent variables. The new variables have been statically condensed at the element level in order to maintain the same number of variables as in the classical quadrilateral RZT element. It has been revealed the great accuracy of these formulated element at an affordable computational cost. Moreover, Thrinth et al. [51] have enhanced the previous higher-order zigzag mixed beam model with the modified stress theory for the analysis of laminated beams, confirming the great improvements in the stress predictions using the HR functional.

In this paper, a new mixed model based on the en-RZT kinematic is formulated to analyse thick multilayered and sandwich structures. The main aim is to obtain an enhanced zigzag plate model that can include the nonlinear distributions of displacements for thick multilayered structures with general lamination schemes. Furthermore, the use of a mixed formulation does not involve the stress recovery technique to describe the correct distribution of the transverse normal and shear stresses. As done by Iurlaro et al. [41] for the original RZT, in this model, the in-plane en-RZT displacement field is enriched with a second and a third order power-series in the thickness coordinate and the transverse displacement is assumed as a second-order polynomial expansion. A new set of higher-order zigzag functions is obtained by enforcing the transverse stress-free condition at top and bottom surfaces, reducing the existing kinematic variables. Moreover, the transverse normal stress is assumed as an independent field, with a smeared cubic through-the-thickness distribution that fulfils the traction boundary conditions on the bottom and top external surfaces. Without using the cylindrical bending assumption and introducing a new set of independent strain variables, the transverse shear stress distributions are derived by using the integration of local equilibrium equations. The Hellinger-Reissner functional is then used to enforce in a weak form the strains compatibility between the strains from the kinematic field and those from the assumed stresses. By following the procedure explained by Auricchio and Sacco [45], a penalty term is added to the energy functional in order to enforce in a weak form the compatibility between the new strain

variables and the strains from the kinematic relations. The new strain variables in conjunction with the penalty functional have been demonstrated [45] for the FSDT to avoid the over-fitting problem in the mixed models. Then, the equilibrium equations and the consistent boundary conditions are derived from the variational functional and specialized for the simply-supported boundary conditions of thick multilayered laminated and sandwich plates under bi-sinusoidal transverse pressure. The accuracy of the proposed model is investigated through a comparison with existing elasticity solutions, when available.

2. The (3,2)-mixed enhanced Refined Zigzag Theory (en-RZT_{{(3,2)}^(m))}

In this Section, the (3,2)-mixed enhanced Refined Zigzag Theory (herein named as en-RZT_{{(3,2)}^(m)) for multilayered composite and sandwich plates is formulated, and the equilibrium equations and consistent boundary conditions are derived.}

2.1. Geometrical preliminaries

We consider a multilayered flat plate made of a finite number N of perfectly bonded layers, V is the volume of the plate and h the total thickness. The points of the plate are referred to an orthogonal Cartesian coordinate system defined by the vector $\mathbf{X} = \{x_i\}$ ($i = 1, 2, 3$), where the

vector $\mathbf{x} = \{x_\alpha\}$ ($\alpha = 1, 2$) is the set of in-plane coordinates on the reference plane, here chosen to be the middle plane of the plate, and x_3 being the co-ordinate normal to the reference plane (see Fig. 1a), so that x_3 is defined in the range $x_3 \in [-\frac{h}{2}, +\frac{h}{2}]$. Let us define $S = S_u \cup S_\sigma$ the total cylindrical edge surface, comprised of S_u , the portion on which displacement restraints are imposed (or prescribed), and S_σ , the portion on which a traction vector, $\bar{\mathbf{F}} = \{\bar{F}_i\}$ ($i = 1, 2, 3$), is prescribed. Moreover, let $\bar{\mathbf{p}}_{(B)} = \{\bar{p}_{i(B)}\}$ and $\bar{\mathbf{p}}_{(T)} = \{\bar{p}_{i(T)}\}$ ($i = 1, 2, 3$) be the vectors of the prescribed tractions on the bottom (B) and top (T) bounding surfaces of the plate, along the coordinate axis x_i . Furthermore, Ω represents the set of points given by the intersection of the plate with the plane $x_3 = 0$ and $\Gamma = S \cap \Omega = \Gamma_u \cup \Gamma_\sigma$ ($\Gamma_u \cap \Gamma_\sigma = \emptyset$) its contour line, with $\Gamma_u = S_u \cap \Omega$ and $\Gamma_\sigma = S_\sigma \cap \Omega$. (See Fig. 1a.)

The thickness of each layer, as well as of the whole plate, is assumed to be constant, and the material of each layer is assumed to be elastic orthotropic with a plane of elastic symmetry parallel to the reference surface and whose principal orthotropy directions are arbitrarily oriented with respect to the in-plane reference frame.

If not otherwise stated, in the paper the superscript (k) is used to indicate quantities corresponding to the k^{th} layer ($k = 1, \dots, N$), whereas the notation $(\cdot)_{(k)}$ ($k = 1, \dots, N-1$) stands for (\cdot) valued for $x_3 = z_{(k)}$, i.e., at the k^{th} interface ($k = 1, \dots, N-1$) between the k^{th} and the $(k + 1)^{\text{th}}$ layer. Also, we use the subscript (B) and (T) to indicate the bottom and top

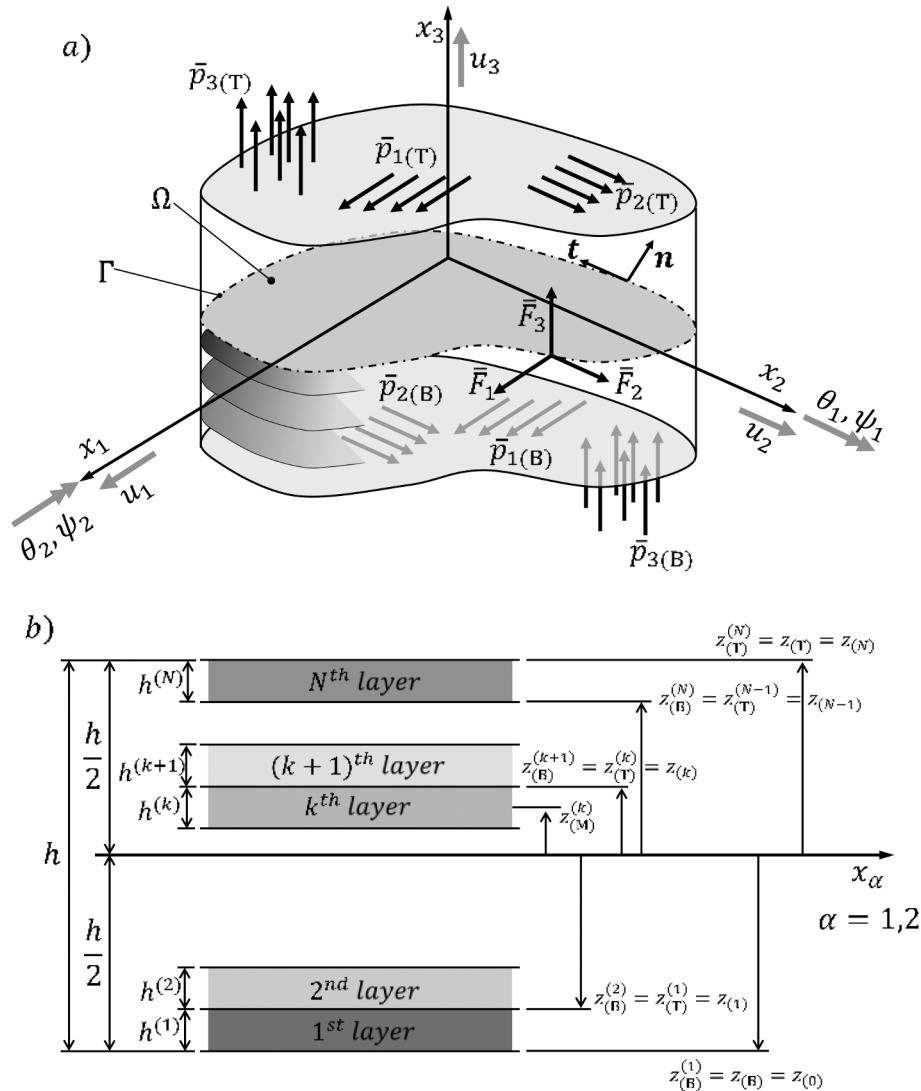


Fig. 1. General plate notation: (a) plate geometry, loads, and coordinate system, (b) layer numbering.

surfaces, respectively, of the single layer/whole plate; specifically, $z_{(B)}^{(1)} = z_{(B)} = -\frac{h}{2}$ and $z_{(T)}^{(N)} = z_{(T)} = \frac{h}{2}$ denote the co-ordinates of the bottom and top surfaces of the whole plate; thus, $h = z_{(T)} - z_{(B)} = z_{(N)} - z_{(0)}$ is the plate thickness and $h^{(k)} = z_{(k)} - z_{(k-1)} = z_{(T)}^{(k)} - z_{(B)}^{(k)}$ ($k = 1, 2, \dots, N$), the thickness of the k^{th} layer (see Fig. 1b).

Furthermore, the symbol $(\cdot)_{,i} = \frac{\partial(\cdot)}{\partial x_i}$ refers to the derivative of the function (\cdot) with respect to the x_i coordinate. In the paper, if not otherwise specified, the Einsteinian summation convention over repeated indices is adopted, with Latin indices ranging from 1 to 3, and Greek indices ranging from 1 to 2.

The prescribed quantities are indicated in the paper with an overbar.

2.2. Kinematic field, strains and stresses

The kinematic field assumption of the en-RZT $_{\{3,2\}}^{(m)}$ involves the use of the en-RZT field for the in-plane displacements in conjunction with a second and third order power-series terms of the thickness coordinate. The transverse displacement is approximated by a second-order power-series expansion in the thickness coordinate. The complete kinematic field can be represented as follows:

$$\begin{aligned} \mathbf{U}^{(k)}(\mathbf{X}) &= \bar{\mathbf{u}}_G(\mathbf{X}) + \bar{\mathbf{u}}_L^{(k)}(\mathbf{X}) \\ U_3(\mathbf{X}) &= w^{(0)}(\mathbf{x}) + zw^{(1)}(\mathbf{x}) + z^2w^{(2)}(\mathbf{x}) \end{aligned} \quad (1)$$

where

$$\begin{aligned} \bar{\mathbf{u}}_G(\mathbf{X}) &= \mathbf{u}(\mathbf{x}) + z\boldsymbol{\theta}(\mathbf{x}) + z^2\boldsymbol{\chi}(\mathbf{x}) + z^3\boldsymbol{\omega}(\mathbf{x}) \\ \bar{\mathbf{u}}_L^{(k)}(\mathbf{X}) &= \boldsymbol{\varphi}^{(k)}(z)\boldsymbol{\Psi}(\mathbf{x}) \end{aligned} \quad (2)$$

$$\begin{aligned} \mathbf{U}^{(k)}(\mathbf{X}) &= \begin{Bmatrix} U_1^{(k)}(\mathbf{X}) \\ U_2^{(k)}(\mathbf{X}) \end{Bmatrix}; \quad \mathbf{u}(\mathbf{x}) = \begin{Bmatrix} u_1(\mathbf{x}) \\ u_2(\mathbf{x}) \end{Bmatrix}; \quad \boldsymbol{\theta}(\mathbf{x}) = \begin{Bmatrix} \theta_1(\mathbf{x}) \\ \theta_2(\mathbf{x}) \end{Bmatrix}; \quad \boldsymbol{\chi}(\mathbf{x}) = \begin{Bmatrix} \chi_1(\mathbf{x}) \\ \chi_2(\mathbf{x}) \end{Bmatrix}; \quad \boldsymbol{\omega}(\mathbf{x}) = \begin{Bmatrix} \omega_1(\mathbf{x}) \\ \omega_2(\mathbf{x}) \end{Bmatrix}; \\ \boldsymbol{\varphi}^{(k)}(z) &= \begin{bmatrix} \phi_{11}^{(k)}(z) & \phi_{12}^{(k)}(z) \\ \phi_{21}^{(k)}(z) & \phi_{22}^{(k)}(z) \end{bmatrix}; \quad \boldsymbol{\Psi}(\mathbf{x}) = \begin{Bmatrix} \psi_1(\mathbf{x}) \\ \psi_2(\mathbf{x}) \end{Bmatrix} \end{aligned} \quad (3)$$

$u_\alpha(\mathbf{x})$ and $\theta_\alpha(\mathbf{x})$ are the global uniform displacements and rotations of the normal to the reference plane about the positive x_2 and the negative x_1 directions, respectively; $\psi_\alpha(\mathbf{x})$ are the zigzag rotations, whereas $\chi_\alpha(\mathbf{x})$, $\omega_\alpha(\mathbf{x})$, $w^{(1)}$ and $w^{(2)}$ are the additional kinematic unknowns that take into account the effect of non-linear distribution of in-plane and transverse displacements along the thickness direction.

Moreover, in Eq. (3) the expression of the linear zigzag functions (such as in Ref. [34]) reads:

$$\boldsymbol{\varphi}^{(k)}(z) = (z - z_{(B)})\boldsymbol{\beta}^{(k)} + \sum_{q=1}^k h^{(q)}(\boldsymbol{\beta}^{(q)} - \boldsymbol{\beta}^{(k)}) \quad (k = 1, \dots, N) \quad (4)$$

where $\boldsymbol{\beta}^{(k)} = \begin{bmatrix} \beta_{11} & \beta_{12} \\ \beta_{21} & \beta_{22} \end{bmatrix}^{(k)}$ is the matrix of zigzag slopes, i.e. $\boldsymbol{\beta}^{(k)}(z) = \boldsymbol{\varphi}_{,z}^{(k)}(z)$, computed by the partial enforcement of the transverse shear stress continuity at the layers interfaces.

Consistent with the linear strain-displacement relations, the en-RZT $_{\{3,2\}}^{(m)}$ strain components can be computed as follows:

$$\begin{aligned} \epsilon_{11}^{(k)}(\mathbf{x}, z) &= U_{1,1}^{(k)}(\mathbf{x}, z); \quad \epsilon_{22}^{(k)}(\mathbf{x}, z) = U_{2,2}^{(k)}(\mathbf{x}, z); \quad \epsilon_{33}(\mathbf{x}, z) = U_{3,3}(\mathbf{x}, z); \\ \gamma_{12}^{(k)}(\mathbf{x}, z) &= U_{1,2}^{(k)}(\mathbf{x}, z) + U_{2,1}^{(k)}(\mathbf{x}, z); \\ \gamma_{13}^{(k)}(\mathbf{x}, z) &= U_{1,3}^{(k)}(\mathbf{x}, z) + U_{3,1}(\mathbf{x}, z); \\ \gamma_{23}^{(k)}(\mathbf{x}, z) &= U_{2,3}^{(k)}(\mathbf{x}, z) + U_{3,2}(\mathbf{x}, z); \end{aligned} \quad (5)$$

Assuming that each layer is linear elastic and orthotropic, as defined by Ref. [42], the mixed constitutive relation written in a convenient form for the formulation of the model can be written as follows

$$\begin{Bmatrix} \sigma_{11}(\mathbf{x}, z) \\ \sigma_{22}(\mathbf{x}, z) \\ \epsilon_{33}(\mathbf{x}, z) \\ \tau_{12}(\mathbf{x}, z) \end{Bmatrix}^{(k)} = \begin{bmatrix} Q_{11} & Q_{12} & R_{13} & Q_{16} \\ Q_{12} & Q_{22} & R_{23} & Q_{26} \\ -R_{13} & -R_{23} & S_{33} & -R_{63} \\ Q_{16} & Q_{26} & R_{63} & Q_{66} \end{bmatrix}^{(k)} \begin{Bmatrix} \epsilon_{11}(\mathbf{x}, z) \\ \epsilon_{22}(\mathbf{x}, z) \\ \sigma_{33}(\mathbf{x}, z) \\ \gamma_{12}(\mathbf{x}, z) \end{Bmatrix}^{(k)} \quad (6)$$

$$\boldsymbol{\tau}_i^{(k)}(\mathbf{x}, z) = \begin{Bmatrix} \tau_{13}(\mathbf{x}, z) \\ \tau_{13}(\mathbf{x}, z) \end{Bmatrix}^{(k)} = \begin{bmatrix} \widehat{C}_{44} & \widehat{C}_{45} \\ \widehat{C}_{45} & \widehat{C}_{55} \end{bmatrix}^{(k)} \begin{Bmatrix} \gamma_{13}(\mathbf{x}, z) \\ \gamma_{13}(\mathbf{x}, z) \end{Bmatrix}^{(k)} = \widehat{\mathbf{C}}_i^{(k)} \boldsymbol{\gamma}_i^{(k)}(\mathbf{x}, z) \quad (7)$$

Where, Q_{ij} ($i, j = 1, 2, 6$) are the in-plane transformed elastic reduced stiffness coefficients; \widehat{C}_{ij} ($i, j = 4, 5$) are the transformed transverse shear elastic stiffness coefficients and $R_{i3} = S_{33}C_{i3}$ ($i = 1, 2, 6$) are transformed mixed coefficients [42].

The kinematics shown in Eq. (1)–(3) involves thirteen unknown variables that are independent by the number of layers. In order to reduce the number of variables, the procedure described by Iurlaro et al. [41] is adopted for condensing some of the global unknowns and introducing a new set of higher-order zigzag functions, that are expected to be piecewise cubic along the thickness direction. In the Section 2.3, the procedure adopted by Iurlaro et al. [41] is applied in a more general

way to the enhanced zigzag functions.

The final reduced kinematic can be expressed as follows:

$$\begin{aligned} \mathbf{U}^{(k)}(\mathbf{x}, z) &= \mathbf{u}_G(\mathbf{x}, z) + \mathbf{u}_L^{(k)}(\mathbf{x}, z) \\ U_3(\mathbf{x}, z) &= w^{(0)}(\mathbf{x}) + zw^{(1)}(\mathbf{x}) + z^2w^{(2)}(\mathbf{x}) \end{aligned} \quad (8)$$

where

$$\begin{aligned} \mathbf{u}_G(\mathbf{x}, z) &= \mathbf{u}(\mathbf{x}) + z\boldsymbol{\theta}(\mathbf{x}) \\ \mathbf{u}_L^{(k)}(\mathbf{x}, z) &= \boldsymbol{\mu}^{(k)}(z)\boldsymbol{\Psi}(\mathbf{x}) \end{aligned} \quad (9)$$

and

$$\boldsymbol{\mu}^{(k)}(z) = \begin{bmatrix} \mu_{11}^{(k)}(z) & \mu_{12}^{(k)}(z) \\ \mu_{21}^{(k)}(z) & \mu_{22}^{(k)}(z) \end{bmatrix} \quad (10)$$

is the new set of higher-order, piecewise cubic zigzag functions, that are null at the top and bottom external surfaces and continuous at the layer interfaces. It should be noted that the coupling extra-diagonal terms in Eq. (10), i.e. $\mu_{12}^{(k)}(z)$ and $\mu_{21}^{(k)}(z)$, are null for cross-ply multilayered and sandwich plates and the expressions for the other functions are the same as those written by Iurlaro [42].

According to the displacement field defined in Eq. (8), by using the strain-displacement relations of Eq. (5), the strains can be defined as

follows;

$$\boldsymbol{\varepsilon}_p^{(k)}(\mathbf{x}, z) = \begin{Bmatrix} \boldsymbol{\varepsilon}_{11}^{(k)}(\mathbf{x}, z) \\ \boldsymbol{\varepsilon}_{22}^{(k)}(\mathbf{x}, z) \\ \boldsymbol{\gamma}_{12}^{(k)}(\mathbf{x}, z) \end{Bmatrix} = \mathbf{I}\boldsymbol{\varepsilon}_m(\mathbf{x}) + z\mathbf{I}\boldsymbol{\varepsilon}_\theta(\mathbf{x}) + \mathbf{M}^{(k)}(z)\boldsymbol{\varepsilon}_\psi(\mathbf{x}) \quad (11)$$

$$\boldsymbol{\varepsilon}_{33}(\mathbf{x}, z) = [0 \ 1 \ 2z] \begin{Bmatrix} w^{(0)}(\mathbf{x}) \\ w^{(1)}(\mathbf{x}) \\ w^{(2)}(\mathbf{x}) \end{Bmatrix} = \mathbf{H}_3^z(z)\mathbf{w}(\mathbf{x})$$

$$\boldsymbol{\gamma}_t^{(k)}(\mathbf{x}, z) = \mathbf{H}^z(z)\partial\mathbf{w}(\mathbf{x}) + \frac{\partial\boldsymbol{\mu}^{(k)}(z)}{\partial z}\boldsymbol{\psi}(\mathbf{x})$$

where \mathbf{I} is the identity matrix, $\mathbf{H}^z(z) = \begin{bmatrix} \widehat{\mathbf{H}}^z(z) & \mathbf{0} \\ \mathbf{0} & \widehat{\mathbf{H}}^z(z) \end{bmatrix}$, $\widehat{\mathbf{H}}^z(z) = [1 \ z \ z^2]$, $\partial\mathbf{w}(\mathbf{x})^T = [w_{,1}^{(0)} \ w_{,1}^{(1)} \ w_{,1}^{(2)} \ w_{,2}^{(0)} \ w_{,2}^{(1)} \ w_{,2}^{(2)}]$ and

$$\mathbf{M}^{(k)}(z) = \begin{bmatrix} \mu_{11}(z) & 0 & 0 & \mu_{12}(z) \\ 0 & \mu_{22}(z) & \mu_{21}(z) & 0 \\ \mu_{21}(z) & \mu_{12}(z) & \mu_{11}(z) & \mu_{22}(z) \end{bmatrix}^{(k)}. \quad \text{Moreover, } \boldsymbol{\varepsilon}_m^T = [u_{1,1} \ u_{2,2} \ u_{1,2} + u_{2,1}], \boldsymbol{\varepsilon}_\theta^T = [\theta_{1,1} \ \theta_{2,2} \ \theta_{1,2} + \theta_{2,1}] \quad \text{and} \quad \boldsymbol{\varepsilon}_\psi^T = [\psi_{1,1} \ \psi_{2,2} \ \psi_{1,2} \ \psi_{2,1}].$$

2.3. Enhanced higher-order zigzag functions

In this Section, the procedure to obtain the enhanced higher-order zigzag functions is shown in details. The expression of transverse shear strains, according to Eq. (5), can be written as follows:

$$\begin{aligned} \boldsymbol{\gamma}_{13}^{(k)}(\mathbf{x}, z) &= U_{3,1}(\mathbf{x}, z) + \theta_1(\mathbf{x}) + 2z\boldsymbol{\chi}_1(\mathbf{x}) + 3z^2\boldsymbol{\omega}_1(\mathbf{x}) + \beta_{11}^{(k)}\boldsymbol{\psi}_1(\mathbf{x}) + \beta_{12}^{(k)}\boldsymbol{\psi}_2(\mathbf{x}) \\ \boldsymbol{\gamma}_{23}^{(k)}(\mathbf{x}, z) &= U_{3,2}(\mathbf{x}, z) + \theta_2(\mathbf{x}) + 2z\boldsymbol{\chi}_2(\mathbf{x}) + 3z^2\boldsymbol{\omega}_2(\mathbf{x}) + \beta_{21}^{(k)}\boldsymbol{\psi}_1(\mathbf{x}) + \beta_{22}^{(k)}\boldsymbol{\psi}_2(\mathbf{x}) \end{aligned} \quad (12)$$

Introducing the definition of the auxiliary strain measure, η_1, η_2 [15]:

$$\begin{aligned} \theta_1(\mathbf{x}) + U_{3,1}(\mathbf{x}, z) - \boldsymbol{\psi}_1 &= \boldsymbol{\gamma}_1(\mathbf{x}) - \boldsymbol{\psi}_1(\mathbf{x}) = \boldsymbol{\eta}_1(\mathbf{x}, z) \\ \theta_2(\mathbf{x}) + U_{3,2}(\mathbf{x}, z) - \boldsymbol{\psi}_2 &= \boldsymbol{\gamma}_2(\mathbf{x}) - \boldsymbol{\psi}_2(\mathbf{x}) = \boldsymbol{\eta}_2(\mathbf{x}, z) \end{aligned} \quad (13)$$

and substituting (13) into Eq. (12), we rewrite:

$$\begin{aligned} \boldsymbol{\gamma}_{13}^{(k)}(\mathbf{x}, z) &= \boldsymbol{\eta}_1(\mathbf{x}, z) + 2z\boldsymbol{\chi}_1(\mathbf{x}) + 3z^2\boldsymbol{\omega}_1(\mathbf{x}) + (\beta_{11}^{(k)} + 1)\boldsymbol{\psi}_1(\mathbf{x}) + \beta_{12}^{(k)}\boldsymbol{\psi}_2(\mathbf{x}) \\ \boldsymbol{\gamma}_{23}^{(k)}(\mathbf{x}, z) &= \boldsymbol{\eta}_2(\mathbf{x}, z) + 2z\boldsymbol{\chi}_2(\mathbf{x}) + 3z^2\boldsymbol{\omega}_2(\mathbf{x}) + \beta_{21}^{(k)}\boldsymbol{\psi}_1(\mathbf{x}) + (\beta_{22}^{(k)} + 1)\boldsymbol{\psi}_2(\mathbf{x}) \end{aligned} \quad (14)$$

In a more convenient matrix form,

$$\begin{Bmatrix} \boldsymbol{\gamma}_{13}^{(k)}(\mathbf{x}, z) \\ \boldsymbol{\gamma}_{23}^{(k)}(\mathbf{x}, z) \end{Bmatrix} = \boldsymbol{\gamma}_t^{(k)}(\mathbf{x}, z) = \boldsymbol{\eta}(\mathbf{x}, z) + 2z\boldsymbol{\chi}(\mathbf{x}) + 3z^2\boldsymbol{\omega}(\mathbf{x}) + (\boldsymbol{\beta}^{(k)}(z) + \mathbf{I})\boldsymbol{\psi}(\mathbf{x}) \quad (15)$$

By using the constitutive relation for material, Eq. (7), and the transverse shear strains in Eq. (15), the transverse shear stresses can be expressed as follows:

$$\begin{aligned} \boldsymbol{\tau}_t^{(k)}(\mathbf{x}, z) &= \widehat{\mathbf{C}}_t^{(k)} [\boldsymbol{\eta}(\mathbf{x}, z) + 2z\boldsymbol{\chi}(\mathbf{x}) + 3z^2\boldsymbol{\omega}(\mathbf{x}) + (\boldsymbol{\beta}^{(k)}(z) + \mathbf{I})\boldsymbol{\psi}(\mathbf{x})] = \\ &= \widehat{\mathbf{C}}_t^{(k)} \boldsymbol{\eta}(\mathbf{x}, z) + \widehat{\mathbf{C}}_t^{(k)} [2z\boldsymbol{\chi}(\mathbf{x}) + 3z^2\boldsymbol{\omega}(\mathbf{x}) + (\boldsymbol{\beta}^{(k)}(z) + \mathbf{I})\boldsymbol{\psi}(\mathbf{x})] = \\ &= {}^d\boldsymbol{\tau}^{(k)}(\mathbf{x}, z) + {}^c\boldsymbol{\tau}^{(k)}(\mathbf{x}, z) \end{aligned} \quad (16)$$

with

$$\begin{aligned} {}^d\boldsymbol{\tau}^{(k)}(\mathbf{x}, z) &= \widehat{\mathbf{C}}_t^{(k)} \boldsymbol{\eta}(\mathbf{x}, z) \\ {}^c\boldsymbol{\tau}^{(k)}(\mathbf{x}, z) &= \widehat{\mathbf{C}}_t^{(k)} [2z\boldsymbol{\chi}(\mathbf{x}) + 3z^2\boldsymbol{\omega}(\mathbf{x}) + (\boldsymbol{\beta}^{(k)}(z) + \mathbf{I})\boldsymbol{\psi}(\mathbf{x})] \end{aligned} \quad (17)$$

By using the same procedure to obtain the zigzag functions formulated for the enhanced-RZT [34], the continuity of the transverse shear stress as defined by Eqs. (16) and (17) is limited to ${}^c\boldsymbol{\tau}^{(k)}(\mathbf{x}, z)$. Thus, the continuity conditions at the N -1 interfaces read as follows:

$$\begin{aligned} \widehat{\mathbf{C}}_t^{(k)} [2z_{(k)}\boldsymbol{\chi}(\mathbf{x}) + 3z_{(k)}^2\boldsymbol{\omega}(\mathbf{x}) + (\boldsymbol{\beta}^{(k)} + \mathbf{I})\boldsymbol{\psi}(\mathbf{x})] \\ = \widehat{\mathbf{C}}_t^{(k+1)} [2z_{(k)}\boldsymbol{\chi}(\mathbf{x}) + 3z_{(k)}^2\boldsymbol{\omega}(\mathbf{x}) + (\boldsymbol{\beta}^{(k+1)} + \mathbf{I})\boldsymbol{\psi}(\mathbf{x})] \end{aligned} \quad (18)$$

In order to reduce the number of variables, the vanishing condition on the top and bottom external surfaces for the continuous part of the transverse shear stresses can be enforced:

$${}^c\boldsymbol{\tau}_{13}^{(k)}(\mathbf{x}, z) \Big|_{z=\pm h/2} = 0; \quad {}^c\boldsymbol{\tau}_{23}^{(k)}(\mathbf{x}, z) \Big|_{z=\pm h/2} = 0 \quad (19)$$

Developing Eq. (19):

$$\begin{aligned} \widehat{\mathbf{C}}_t^{(1)} \left[-h\boldsymbol{\chi}(\mathbf{x}) + \frac{3}{4}h^2\boldsymbol{\omega}(\mathbf{x}) + (\boldsymbol{\beta}^{(1)} + \mathbf{I})\boldsymbol{\psi}(\mathbf{x}) \right] &= \mathbf{0} \\ \widehat{\mathbf{C}}_t^{(N)} \left[h\boldsymbol{\chi}(\mathbf{x}) + \frac{3}{4}h^2\boldsymbol{\omega}(\mathbf{x}) + (\boldsymbol{\beta}^{(N)} + \mathbf{I})\boldsymbol{\psi}(\mathbf{x}) \right] &= \mathbf{0} \end{aligned} \quad (20)$$

After some mathematical manipulations, here not reported for sake of brevity, the following relations are obtained:

$$\begin{aligned} \boldsymbol{\omega}(\mathbf{x}) &= -\frac{(\boldsymbol{\beta}^{(1)} + \boldsymbol{\beta}^{(N)} + 2\mathbf{I})}{\frac{3}{2}h^2}\boldsymbol{\psi}(\mathbf{x}) = -\boldsymbol{\omega}_0\boldsymbol{\psi}(\mathbf{x}) \\ \boldsymbol{\chi}(\mathbf{x}) &= -\frac{1}{2h}(\boldsymbol{\beta}^{(N)} - \boldsymbol{\beta}^{(1)})\boldsymbol{\psi}(\mathbf{x}) = -\boldsymbol{\chi}_0\boldsymbol{\psi}(\mathbf{x}) \end{aligned} \quad (21)$$

The relations in Eq. (21) allow to reduce the number of kinematic variables, relating the new one introduced for the parabolic and cubic terms in the in-plane displacement field to the zigzag rotations.

By substituting the relations of Eq. (21) into the kinematic field of Eq. (1), the reduced kinematic field can be obtained as shown in Eqs. (8) and (9), where the higher-order zigzag functions are defined as follows:

$$\boldsymbol{\mu}^{(k)}(z) = (-z^2\boldsymbol{\chi}_0 - z^3\boldsymbol{\omega}_0 + \boldsymbol{\varphi}^{(k)}(z)) \quad (22)$$

It can be noted that the new set of higher-order zigzag functions are dependent on the thickness coordinate and on the linear zigzag slopes, i. e. $\boldsymbol{\beta}^{(k)}$. In order to compute the $\boldsymbol{\beta}^{(k)}$ values for each layer, Eq. (18) is enforced at each layer interfaces. The last conditions required to completely define the functions in Eq. (22) is the zero values of on the top/bottom external surface of the higher-order zigzag functions. Thus,

$$\boldsymbol{\mu}^{(1)}(z = -h/2) = \boldsymbol{\mu}^{(N)}(z = +h/2) = \mathbf{0} \quad (23)$$

2.4. Assumed transverse normal stress

In this Section, the assumed transverse normal stress is defined and briefly described.

The transverse normal stress is assumed as a third-order power function of the transverse coordinate [40]:

$$\sigma_{33}^a(\mathbf{x}, z) = \sigma_0^a(\mathbf{x}) + z\sigma_1^a(\mathbf{x}) + z^2\sigma_2^a(\mathbf{x}) + z^3\sigma_3^a(\mathbf{x}) \quad (24)$$

Enforcing at the top and bottom external surfaces the traction boundary conditions, i.e.

$$\begin{aligned} \sigma_{33}^a(\mathbf{x}, z = -h/2) &= -\bar{p}_{3(B)} \\ \sigma_{33}^a(\mathbf{x}, z = h/2) &= \bar{p}_{3(T)} \end{aligned} \quad (25)$$

and after some straightforward manipulations, the assumed transverse normal stress is written as follows:

$$\sigma_{33}^a(\mathbf{x}, z) = \mathbf{P}_\sigma(z)\mathbf{q}_\sigma(\mathbf{x}) + \mathbf{L}(z)\bar{\mathbf{q}}_z(\mathbf{x}) \quad (26)$$

where

$$\mathbf{L}(z) = \left[\left(\frac{z}{h} - \frac{1}{2} \right) \quad \left(\frac{z}{h} + \frac{1}{2} \right) \right]; \quad \mathbf{P}_\sigma(z) = \left[\left(z^2 - \frac{h^2}{4} \right) \quad z \left(z^2 - \frac{h^2}{4} \right) \right];$$

$$\bar{\mathbf{q}}_z(\mathbf{x})^T = [\bar{p}_{3(B)} \quad \bar{p}_{3(T)}]; \quad \mathbf{q}_\sigma(\mathbf{x})^T = [\sigma_z^c \quad \sigma_z^s]$$
(27)

2.5. Assumed transverse shear stresses

The assumed transverse shear stresses, following the formulation proposed by Auricchio and Sacco [45], is derived by the integration of the local three-dimensional equilibrium equations, i.e.

$$\sigma_{11,1}^{(k)}(\mathbf{x}, z) + \tau_{12,2}^{(k)}(\mathbf{x}, z) + \tau_{13,3}^{(k)}(\mathbf{x}, z) = 0$$

$$\tau_{12,1}^{(k)}(\mathbf{x}, z) + \sigma_{22,2}^{(k)}(\mathbf{x}, z) + \tau_{23,3}^{(k)}(\mathbf{x}, z) = 0$$
(28)

According to the derivation reported in [45], the assumed transverse shear stresses are deduced by Eq. (28) in which the in-plane stresses are those coming from the constitutive relation expressed in Eq. (6), but the strains quantities are assumed independently with respect to the kinematic field. This assumption can be reported as follows:

$$\boldsymbol{\varepsilon}_p^{(k)}(\mathbf{x}, z) = \mathbf{I}\mathbf{e}_m(\mathbf{x}) + z\mathbf{I}\mathbf{e}_\theta(\mathbf{x}) + \mathbf{M}^{(k)}(z)\boldsymbol{\varepsilon}_\psi(\mathbf{x}) \rightarrow$$

$$\rightarrow \mathbf{I}\mathbf{e}(\mathbf{x}) + z\mathbf{I}\mathbf{k}(\mathbf{x}) + \mathbf{M}^{(k)}(z)\mathbf{k}^\psi(\mathbf{x})$$
(29)

where the vectors of the new assumed strain variables are defined as follows: $\mathbf{e}^T = [e_{11} \quad e_{22} \quad e_{12}]$; $\mathbf{k}^T = [k_{11} \quad k_{22} \quad k_{12}]$; $\mathbf{k}^{\psi T} = [k_{11}^\psi \quad k_{22}^\psi \quad k_{12}^\psi \quad k_{21}^\psi]$.

The new independent expressions for strain quantities are then used in combination with the constitutive relation Eq. (6), and the Eq. (28). After some mathematical passages reported in the Appendix B for sake of brevity, the final expression of the assumed transverse shear stresses is:

$$\boldsymbol{\tau}_t^a(\mathbf{x}, z) = \mathbf{Z}_p(z)\bar{\mathbf{q}}_p(\mathbf{x}) + \mathbf{Z}_t(z)\mathbf{q}_t(\mathbf{x}) + \mathbf{Z}_{qz}(z)\partial\bar{\mathbf{q}}_z(\mathbf{x})$$
(30)

where $\partial\bar{\mathbf{q}}_z(\mathbf{x})$ represent the derivatives of the transverse distributed load, i.e. $\partial\bar{\mathbf{q}}_z(\mathbf{x})^T = [\bar{p}_{3(B),1} \quad \bar{p}_{3(B),2} \quad \bar{p}_{3(T),1} \quad \bar{p}_{3(T),2}]$; $\bar{\mathbf{q}}_p(\mathbf{x})$ is the vector of the prescribed tractions in the x_1 and x_2 direction at the bottom and top external surfaces, i.e. $\bar{\mathbf{q}}_p(\mathbf{x})^T = [\bar{p}_{1(B)} \quad \bar{p}_{2(B)} \quad \bar{p}_{1(T)} \quad \bar{p}_{2(T)}]$; $\mathbf{q}_t(\mathbf{x})^T = [\partial\mathbf{e}(\mathbf{x})^T \quad \partial\mathbf{k}(\mathbf{x})^T \quad \partial\mathbf{k}^\psi(\mathbf{x})^T \quad \partial\mathbf{w}(\mathbf{x})^T]$ is the vector of the derivatives of the strain unknowns, their full expressions are reported in Appendix B.

2.6. Variational statement, equilibrium equations and boundary conditions

In this Section, the en-RZT_{3,2}^(m) is developed by using the variational statement as described by Auricchio and Sacco [45]. Neglecting the virtual work done by the inertia forces, the first term ($\delta\Pi_{\text{int}}$) is the work done by the internal stresses. The second term ($\delta\Pi_{\text{HR}}$), related to the transverse shear and transverse normal stress is represented by the Hellinger-Reissner (HR) functional in which the weak compatibility constraint for the transverse strains obtained by the assumed independent stress fields, as it has been shown by Eqs. (26) and (30), has been enforced. Since the assumed transverse shear stresses are dependent on the new strains quantities, a new penalty functional is added to the variational statement ($\delta\Lambda$). This penalty term guarantees the weak

enforcement of the compatibility relations between the strains coming from the displacement field and the new independent strain variables. According to these assumption the variational statement can read as follows:

$$\delta\Pi = \delta\Pi_{\text{int}} + \delta\Pi_{\text{HR}} + \delta\Lambda - \delta\Pi_{\text{ext}} = 0$$
(31)

where $\delta\Pi_{\text{int}}$ is the virtual work done by the internal stresses defined as follows:

$$\delta\Pi_{\text{int}} = \int_V \left[(\delta\boldsymbol{\varepsilon}_p^{(k)T} \boldsymbol{\sigma}_p^{(k)} + \delta\boldsymbol{\gamma}_t^{(k)T} \boldsymbol{\tau}_t^a + \delta\varepsilon_{33} \sigma_{33}^a) \right] dV$$
(32)

$\delta\Pi_{\text{HR}}$ is the virtual variation of the Hellinger-Reissner functional for the transverse shear and the transverse normal stress and it reads:

$$\delta\Pi_{\text{HR}} = \int_V \left[\delta\boldsymbol{\tau}_t^{aT} (\boldsymbol{\gamma}_t^{(k)} - \boldsymbol{\gamma}_t^{(k)a}) + \delta\sigma_{33}^a (\varepsilon_{33} - \varepsilon_{33}^{(k)a}) \right] dV$$
(33)

$\delta\Lambda$ is the virtual variation of the penalty functional, introduced to assure the compatibility condition between the assumed strain field and the strains obtained by the assumed displacement field. Thus, it reads:

$$\delta\Lambda = \frac{1}{\eta} \int_V \left[(\delta\boldsymbol{\varepsilon}_m - \delta\mathbf{e})^T (\boldsymbol{\varepsilon}_m - \mathbf{e}) + (\delta\boldsymbol{\varepsilon}_\theta - \delta\mathbf{k})^T (\boldsymbol{\varepsilon}_\theta - \mathbf{k}) + (\delta\boldsymbol{\varepsilon}_\psi - \delta\mathbf{k}^\psi)^T (\boldsymbol{\varepsilon}_\psi - \mathbf{k}^\psi) \right] dV$$
(34)

$\delta\Pi_{\text{ext}}$ is the virtual variation of the external applied traction loads (the traction forces $\bar{\mathbf{F}}$ are neglected):

$$\delta\Pi_{\text{ext}} = \int_\Omega \bar{p}_{1(T)} U_1^{(N)}(z = h/2) d\Omega + \int_\Omega \bar{p}_{1(B)} U_1^{(1)}(z = -h/2) d\Omega$$

$$+ \int_\Omega \bar{p}_{2(T)} U_2^{(N)}(z = h/2) d\Omega + \int_\Omega \bar{p}_{2(B)} U_2^{(1)}(z = -h/2) d\Omega +$$

$$+ \int_\Omega \bar{p}_{3(T)} U_3^{(N)}(z = h/2) d\Omega + \int_\Omega \bar{p}_{3(B)} U_3^{(1)}(z = -h/2) d\Omega +$$
(35)

In the previous expressions, the a superscript denotes the quantities related to the assumed fields and δ defines the arbitrary virtual variation. η is the penalty parameter in the penalty functional. As defined by Eq. (11), in Eq. (32), $\boldsymbol{\varepsilon}_p^{(k)T} = [e_{11}^{(k)} \quad e_{22}^{(k)} \quad \gamma_{12}^{(k)}]$ is the vector of in-plane strains obtained by the displacement field; $\boldsymbol{\sigma}_p^{(k)T} = [\sigma_{11}^{(k)} \quad \sigma_{22}^{(k)} \quad \tau_{12}^{(k)}]$ is the vector of in-plane stresses; $\boldsymbol{\gamma}_t^{(k)T} = [\gamma_{13}^{(k)} \quad \gamma_{23}^{(k)}]$ is the vector of the transverse shear strains computed by the assumed displacement field and ε_{33} is the transverse normal strain according to the strain-displacement relations.

In virtue of the independent assumption of the kinematics, Eq. (8), and the transverse normal stress, Eq. (26), the variational statement can be split into two contributions:

$$\delta\Pi_{\sigma_z} = \int_V \left[\delta\sigma_{33}^a (\varepsilon_{33} - \varepsilon_{33}^{(k)a}) \right] dV$$
(36)

and

$$\int_V \left[(\delta\boldsymbol{\varepsilon}_p^{(k)T} \boldsymbol{\sigma}_p^{(k)} + \delta\boldsymbol{\gamma}_t^{(k)T} \boldsymbol{\tau}_t^a + \delta\varepsilon_{33} \sigma_{33}^a) \right] dV + \int_V \delta\boldsymbol{\tau}_t^{aT} (\boldsymbol{\gamma}_t^{(k)} - \boldsymbol{\gamma}_t^{(k)a}) dV +$$

$$+ \frac{1}{\eta} \int_V \left[(\delta\boldsymbol{\varepsilon}_m - \delta\mathbf{e})^T (\boldsymbol{\varepsilon}_m - \mathbf{e}) + (\delta\boldsymbol{\varepsilon}_\theta - \delta\mathbf{k})^T (\boldsymbol{\varepsilon}_\theta - \mathbf{k}) + (\delta\boldsymbol{\varepsilon}_\psi - \delta\mathbf{k}^\psi)^T (\boldsymbol{\varepsilon}_\psi - \mathbf{k}^\psi) \right] dV - \delta\Pi_{\text{ext}} = 0$$
(37)

that can be solved separately. Firstly, Eq. (36) is solved as a weak form compatibility constraint between the transverse normal strain expressed in terms of the kinematic variables and that coming from the assumed transverse normal stress. Secondly, Eq. (37) is solved. It represents the variational expression of the work done by strains and stresses and that done by external forces, and it contains a contribution deriving from the weak form compatibility constraint between the transverse shear strains plus the penalty constraint of the strains quantities. Performing the integration by parts, it results into the governing equations with the variationally consistent boundary conditions.

According to the procedure, the Eq. (36) is solved (for sake of brevity, the final results are here reported, for more details refer to Appendix A) and the assumed transverse normal stress has the following expression:

$$\sigma_{33}^a(\mathbf{x}, z) = \mathbf{A}_\sigma^u(z)\boldsymbol{\varepsilon}_m(\mathbf{x}) + \mathbf{A}_\sigma^\theta(z)\boldsymbol{\varepsilon}_\theta(\mathbf{x}) + \mathbf{A}_\sigma^\psi(z)\boldsymbol{\varepsilon}_\psi(\mathbf{x}) + \mathbf{A}_\sigma^w(z)\mathbf{w}(\mathbf{x}) + \mathbf{A}_\sigma^{qz}(z)\bar{\mathbf{q}}_z(\mathbf{x}) \quad (38)$$

where $\mathbf{A}_\sigma^u(z)$, $\mathbf{A}_\sigma^\theta(z)$, $\mathbf{A}_\sigma^\psi(z)$, $\mathbf{A}_\sigma^w(z)$, $\mathbf{A}_\sigma^{qz}(z)$ are the shape functions of the transverse coordinate and their definition is reported in Appendix A.

By introducing the assumed transverse normal stress defined by Eq. (38) and the assumed transverse shear stresses defined by Eq. (30) into the variational statement (37), and performing the conventional integration by parts, the governing equations of the en-RZT_(3,2)^(m) plate can be obtained as follows (the full expression of the terms are reported in Appendix C):

$$\delta u_1 : N_{11,1} + N_{12,2} + \frac{1}{\eta}(u_{1,11} - e_{11,1}) + \frac{1}{\eta}(u_{1,22} + u_{2,12} - e_{12,2}) + \bar{p}_1 = 0 \quad (39)$$

$$\delta u_2 : N_{12,1} + N_{22,2} + \frac{1}{\eta}(v_{,yy} - e_{22,y}) + \frac{1}{\eta}(u_{1,12} + u_{2,11} - e_{12,1}) + \bar{p}_2 = 0 \quad (40)$$

$$\begin{aligned} \delta \theta_y : M_{12,1} + M_{22,2} - Q_2 + \frac{1}{\eta}(\theta_{2,22} - k_{22,2}) + \frac{1}{\eta}(\theta_{1,12} + \theta_{2,11} - k_{12,1}) + \bar{m}_2 \\ = 0 \end{aligned} \quad (45)$$

$$\delta \psi_x : M_{11,1}^\psi + M_{12,2}^\psi - Q_1^\psi + \frac{1}{\eta}(\psi_{1,11} - k_{11,1}^\psi) + \frac{1}{\eta}(\psi_{1,22} - k_{12,2}^\psi) = 0 \quad (46)$$

$$\delta \psi_y : M_{21,1}^\psi + M_{22,2}^\psi - Q_2^\psi + \frac{1}{\eta}(\psi_{2,22} - k_{22,2}^\psi) + \frac{1}{\eta}(\psi_{2,11} - k_{21,1}^\psi) = 0 \quad (47)$$

$$\delta e_{11} : -\frac{1}{\eta}(e_{11} - u_{1,1}) + E_{11}^{HR} = 0 \quad (48)$$

$$\delta e_{22} : -\frac{1}{\eta}(e_{22} - u_{2,2}) + E_{22}^{HR} = 0 \quad (49)$$

$$\delta e_{12} : -\frac{1}{\eta}(e_{12} - u_{1,2} - u_{2,1}) + E_{12}^{HR} = 0 \quad (50)$$

$$\delta k_{11} : -\frac{1}{\eta}(k_{11} - \theta_{1,1}) + K_{11}^{HR} = 0 \quad (51)$$

$$\delta k_{22} : -\frac{1}{\eta}(k_{22} - \theta_{2,2}) + K_{22}^{HR} = 0 \quad (52)$$

$$\delta k_{12} : -\frac{1}{\eta}(k_{12} - \theta_{1,2} - \theta_{2,1}) + K_{12}^{HR} = 0 \quad (53)$$

$$\delta k_{11}^\psi : -\frac{1}{\eta}(k_{11}^\psi - \psi_{1,1}) + K_{\psi 11}^{HR} = 0 \quad (54)$$

$$\delta k_{22}^\psi : -\frac{1}{\eta}(k_{22}^\psi - \psi_{2,2}) + K_{\psi 22}^{HR} = 0 \quad (55)$$

$$\begin{aligned} \delta w^{(0)} : Q_{1,1}^{w0} + Q_{2,2}^{w0} - N_3^{\tilde{}} - \tilde{Q}^{w0} + \\ - \left(\hat{D}_{11}^p \bar{p}_{1(B),1} + \hat{D}_{12}^p \bar{p}_{2(B),1} + \hat{D}_{13}^p \bar{p}_{1(T),1} + \hat{D}_{14}^p \bar{p}_{2(T),1} + \hat{D}_{41}^p \bar{p}_{1(B),2} + \hat{D}_{42}^p \bar{p}_{2(B),2} + \hat{D}_{43}^p \bar{p}_{1(T),2} + \hat{D}_{44}^p \bar{p}_{2(T),2} \right) + \\ - \left(\hat{D}_{41}^q \bar{p}_{3(B),12} + \hat{D}_{42}^q \bar{p}_{3(T),12} + \hat{D}_{43}^q \bar{p}_{3(B),22} + \hat{D}_{44}^q \bar{p}_{3(T),22} + \hat{D}_{11}^q \bar{p}_{3(B),11} + \hat{D}_{12}^q \bar{p}_{3(T),11} + \hat{D}_{13}^q \bar{p}_{3(B),12} + \hat{D}_{14}^q \bar{p}_{3(T),12} \right) + \bar{q}_3 = 0 \end{aligned} \quad (41)$$

$$\begin{aligned} \delta w^{(1)} : Q_{1,1}^{w1} + Q_{2,2}^{w1} - N_3^{\tilde{}} - \tilde{Q}^{w1} + \\ - \left(\hat{D}_{21}^p \bar{p}_{1(B),1} + \hat{D}_{22}^p \bar{p}_{2(B),1} + \hat{D}_{23}^p \bar{p}_{1(T),1} + \hat{D}_{24}^p \bar{p}_{2(T),1} + \hat{D}_{51}^p \bar{p}_{1(B),2} + \hat{D}_{52}^p \bar{p}_{2(B),2} + \hat{D}_{53}^p \bar{p}_{1(T),2} + \hat{D}_{54}^p \bar{p}_{2(T),2} \right) + \\ - \left(\hat{D}_{11}^q \bar{p}_{3(B),11} + \hat{D}_{12}^q \bar{p}_{3(T),11} + \hat{D}_{13}^q \bar{p}_{3(B),12} + \hat{D}_{14}^q \bar{p}_{3(T),12} + \hat{D}_{51}^q \bar{p}_{3(B),12} + \hat{D}_{52}^q \bar{p}_{3(T),12} + \hat{D}_{53}^q \bar{p}_{3(B),22} + \hat{D}_{54}^q \bar{p}_{3(T),22} \right) + \frac{h}{2}(\bar{p}_{3(T)} - \bar{p}_{3(B)}) = 0 \end{aligned} \quad (42)$$

$$\begin{aligned} \delta w^{(2)} : Q_{1,1}^{w2} + Q_{2,2}^{w2} - N_3^{\tilde{}} - \tilde{Q}^{w2} + \\ - \left(\hat{D}_{31}^p \bar{p}_{1(B),1} + \hat{D}_{32}^p \bar{p}_{2(B),1} + \hat{D}_{33}^p \bar{p}_{1(T),1} + \hat{D}_{34}^p \bar{p}_{2(T),1} + \hat{D}_{61}^p \bar{p}_{1(B),2} + \hat{D}_{62}^p \bar{p}_{2(B),2} + \hat{D}_{63}^p \bar{p}_{1(T),2} + \hat{D}_{64}^p \bar{p}_{2(T),2} \right) + \\ - \left(\hat{D}_{31}^q \bar{p}_{3(B),11} + \hat{D}_{32}^q \bar{p}_{3(T),11} + \hat{D}_{33}^q \bar{p}_{3(B),12} + \hat{D}_{34}^q \bar{p}_{3(T),12} + \hat{D}_{61}^q \bar{p}_{3(B),12} + \hat{D}_{62}^q \bar{p}_{3(T),12} + \hat{D}_{63}^q \bar{p}_{3(B),22} + \hat{D}_{64}^q \bar{p}_{3(T),22} \right) + \frac{h^2}{4}\bar{q}_3 = 0 \end{aligned} \quad (43)$$

$$\delta k_{12}^\psi : -\frac{1}{\eta}(k_{12}^\psi - \psi_{1,2}) + K_{\psi 12}^{HR} = 0 \quad (56)$$

$$\delta k_{21}^\psi : -\frac{1}{\eta}(k_{21}^\psi - \psi_{2,1}) + K_{\psi 21}^{HR} = 0 \quad (57)$$

The consistent boundary conditions are (for sake of brevity, the full expressions of some terms are reported in the Appendix C):

expressions for the assumed transverse normal and shear stresses, i.e. Eqs. (38) and (30), the following constitutive relations for the en-

$$\begin{aligned}
 u_1 = \bar{u}_1 & \quad \text{on } \Gamma_u & \vee & \quad \bar{N}_{11}n_1 + \bar{N}_{12}n_2 + \frac{1}{\eta}(u_{1,1} - e_{11})n_1 + \frac{1}{\eta}(u_{1,2} + u_{2,1} - e_{12})n_2 & \quad \text{on } \Gamma_\sigma \\
 u_2 = \bar{u}_2 & \quad \text{on } \Gamma_u & \vee & \quad \bar{N}_{12}n_1 + \bar{N}_{22}n_2 + \frac{1}{\eta}(u_{2,2} - e_{22})n_2 + \frac{1}{\eta}(u_{1,2} + u_{2,1} - e_{12})n_1 & \quad \text{on } \Gamma_\sigma \\
 w^{(0)} = \bar{w}^{(0)} & \quad \text{on } \Gamma_u & \vee & \quad \bar{Q}_1^{w0}n_1 + \bar{Q}_2^{w0}n_2 + \frac{HR}{\eta}\bar{Q}_1^{w0}n_1 + \frac{HR}{\eta}\bar{Q}_2^{w0}n_2 & \quad \text{on } \Gamma_\sigma \\
 w^{(1)} = \bar{w}^{(1)} & \quad \text{on } \Gamma_u & \vee & \quad \bar{Q}_1^{w1}n_1 + \bar{Q}_2^{w1}n_2 + \frac{HR}{\eta}\bar{Q}_1^{w1}n_1 + \frac{HR}{\eta}\bar{Q}_2^{w1}n_2 & \quad \text{on } \Gamma_\sigma \\
 w^{(2)} = \bar{w}^{(2)} & \quad \text{on } \Gamma_u & \vee & \quad \bar{Q}_1^{w2}n_1 + \bar{Q}_2^{w2}n_2 + \frac{HR}{\eta}\bar{Q}_1^{w2}n_1 + \frac{HR}{\eta}\bar{Q}_2^{w2}n_2 & \quad \text{on } \Gamma_\sigma \\
 \theta_1 = \bar{\theta}_1 & \quad \text{on } \Gamma_u & \vee & \quad \bar{M}_{11}n_1 + \bar{M}_{12}n_2 + \frac{1}{\eta}(\theta_{1,1} - k_{11})n_1 + \frac{1}{\eta}(\theta_{1,2} + \theta_{2,1} - k_{12})n_2 & \quad \text{on } \Gamma_\sigma \\
 \theta_2 = \bar{\theta}_2 & \quad \text{on } \Gamma_u & \vee & \quad \bar{M}_{12}n_1 + \bar{M}_{22}n_2 + \frac{1}{\eta}(\theta_{2,2} - k_{22})n_2 + \frac{1}{\eta}(\theta_{1,2} + \theta_{2,1} - k_{12})n_1 & \quad \text{on } \Gamma_\sigma \\
 \psi_1 = \bar{\psi}_1 & \quad \text{on } \Gamma_u & \vee & \quad \bar{M}_{11}^\psi n_1 + \bar{M}_{12}^\psi n_2 + \frac{1}{\eta}(\psi_{1,1} - k_{11}^\psi)n_1 + \frac{1}{\eta}(\psi_{1,2} - k_{12}^\psi)n_2 & \quad \text{on } \Gamma_\sigma \\
 \psi_2 = \bar{\psi}_2 & \quad \text{on } \Gamma_u & \vee & \quad \bar{M}_{21}^\psi n_1 + \bar{M}_{22}^\psi n_2 + \frac{1}{\eta}(\psi_{2,2} - k_{22}^\psi)n_2 + \frac{1}{\eta}(\psi_{2,1} - k_{21}^\psi)n_1 & \quad \text{on } \Gamma_\sigma \\
 e_{11} = \bar{e}_{11} & \quad \text{on } \Gamma_u & \vee & \quad \frac{HR}{E_1}e_{11}n_1 + \frac{HR}{E_2}e_{11}n_2 & \quad \text{on } \Gamma_\sigma \\
 e_{22} = \bar{e}_{22} & \quad \text{on } \Gamma_u & \vee & \quad \frac{HR}{E_1}e_{22}n_1 + \frac{HR}{E_2}e_{22}n_2 & \quad \text{on } \Gamma_\sigma \\
 e_{12} = \bar{e}_{12} & \quad \text{on } \Gamma_u & \vee & \quad \frac{HR}{E_1}e_{12}n_1 + \frac{HR}{E_2}e_{12}n_2 & \quad \text{on } \Gamma_\sigma \\
 k_{11} = \bar{k}_{11} & \quad \text{on } \Gamma_u & \vee & \quad \frac{HR}{K_1}k_{11}n_1 + \frac{HR}{K_2}k_{11}n_2 & \quad \text{on } \Gamma_\sigma \\
 k_{22} = \bar{k}_{22} & \quad \text{on } \Gamma_u & \vee & \quad \frac{HR}{K_1}k_{22}n_1 + \frac{HR}{K_2}k_{22}n_2 & \quad \text{on } \Gamma_\sigma \\
 k_{12} = \bar{k}_{12} & \quad \text{on } \Gamma_u & \vee & \quad \frac{HR}{K_1}k_{12}n_1 + \frac{HR}{K_2}k_{12}n_2 & \quad \text{on } \Gamma_\sigma \\
 k_{11}^\psi = \bar{k}_{11}^\psi & \quad \text{on } \Gamma_u & \vee & \quad \frac{HR}{K_1}k_{11}^\psi n_1 + \frac{HR}{K_2}k_{11}^\psi n_2 & \quad \text{on } \Gamma_\sigma \\
 k_{22}^\psi = \bar{k}_{22}^\psi & \quad \text{on } \Gamma_u & \vee & \quad \frac{HR}{K_1}k_{22}^\psi n_1 + \frac{HR}{K_2}k_{22}^\psi n_2 & \quad \text{on } \Gamma_\sigma \\
 k_{12}^\psi = \bar{k}_{12}^\psi & \quad \text{on } \Gamma_u & \vee & \quad \frac{HR}{K_1}k_{12}^\psi n_1 + \frac{HR}{K_2}k_{12}^\psi n_2 & \quad \text{on } \Gamma_\sigma \\
 k_{21}^\psi = \bar{k}_{21}^\psi & \quad \text{on } \Gamma_u & \vee & \quad \frac{HR}{K_1}k_{21}^\psi n_1 + \frac{HR}{K_2}k_{21}^\psi n_2 & \quad \text{on } \Gamma_\sigma
 \end{aligned} \tag{58}$$

In Eq. (58), $n_1 = \cos(x_1, n)$ and $n_2 = \cos(x_2, n)$ are the components (direction cosines) of the unit outward normal vector to the cylindrical plate edges.

The resultant forces and moments are defined as:

$$\begin{aligned}
 (\mathbf{N}, \mathbf{M}, \mathbf{M}^\psi) &= \int_{-h/2}^{+h/2} (1, z, \mathbf{M}^{(k)T}) \boldsymbol{\sigma}_p^{(k)} dz; \\
 \mathbf{N}^z &= \int_{-h/2}^{+h/2} \mathbf{H}_{;3}^T \sigma_{33}^a dz \\
 (\mathbf{Q}^w, \mathbf{Q}, \mathbf{Q}^\psi) &= \int_{-h/2}^{+h/2} (\mathbf{H}^{cT}, \mathbf{I}, \partial \boldsymbol{\mu}_z^T) \boldsymbol{\tau}_t^a dz
 \end{aligned} \tag{59}$$

Moreover, in Eqs. (39)–(45),

$$\begin{aligned}
 \bar{p}_1 &= \bar{p}_{1(B)} + \bar{p}_{1(T)}; \quad \bar{p}_2 = \bar{p}_{2(B)} + \bar{p}_{2(T)}; \\
 \bar{m}_1 &= \frac{h}{2} (\bar{p}_{1(T)} - \bar{p}_{1(B)}); \quad \bar{m}_2 = \frac{h}{2} (\bar{p}_{2(T)} - \bar{p}_{2(B)}); \\
 \bar{q}_3 &= \bar{q}_{3(B)} + \bar{q}_{3(T)}
 \end{aligned} \tag{60}$$

By using the mixed material constitutive relations, i.e. (6), and the

$\text{RZT}_{\{3,2\}}^{(m)}$, are expressed as follows:

$$\mathbf{N} = \tilde{\mathbf{A}} \boldsymbol{\varepsilon}_m + \tilde{\mathbf{B}} \boldsymbol{\varepsilon}_\theta + \tilde{\mathbf{A}}^\psi \boldsymbol{\varepsilon}_\psi + \tilde{\mathbf{A}}^w \mathbf{w} + \tilde{\mathbf{A}}^{qz} \bar{\mathbf{q}}_z \tag{61}$$

$$\mathbf{M} = \tilde{\mathbf{C}} \boldsymbol{\varepsilon}_m + \tilde{\mathbf{D}} \boldsymbol{\varepsilon}_\theta + \tilde{\mathbf{B}}^\psi \boldsymbol{\varepsilon}_\psi + \tilde{\mathbf{B}}^w \mathbf{w} + \tilde{\mathbf{B}}^{qz} \bar{\mathbf{q}}_z \tag{61}$$

$$\mathbf{M}^\psi = \tilde{\mathbf{E}}^\psi \boldsymbol{\varepsilon}_m + \tilde{\mathbf{F}}^\psi \boldsymbol{\varepsilon}_\theta + \tilde{\mathbf{G}}^\psi \boldsymbol{\varepsilon}_\psi + \tilde{\mathbf{C}}^w \mathbf{w} + \tilde{\mathbf{C}}^{qz} \bar{\mathbf{q}}_z \tag{62}$$

$$\mathbf{N}^z = \mathbf{A}^{Nz} \boldsymbol{\varepsilon}_m + \mathbf{B}^{Nz} \boldsymbol{\varepsilon}_\theta + \mathbf{C}^{Nz} \boldsymbol{\varepsilon}_\psi + \mathbf{D}^{Nz} \mathbf{w} + \mathbf{E}^{Nz} \bar{\mathbf{q}}_z \tag{62}$$

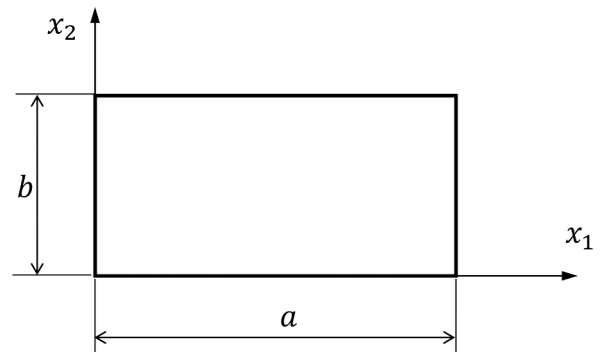


Fig. 2. Rectangular plate dimensions and coordinate system.

$$\begin{aligned}
 \mathbf{Q}^w &= \widehat{\mathbf{A}}^{wT} \partial \mathbf{e} + \widehat{\mathbf{B}}^{wT} \partial \mathbf{k} + \widehat{\mathbf{C}}^{wT} \partial \mathbf{k}^\psi + \widehat{\mathbf{D}}^{wT} \partial \mathbf{w} + \widehat{\mathbf{E}}^w \partial \bar{\mathbf{q}}_z \\
 \mathbf{Q} &= \widehat{\mathbf{A}}^{\theta T} \partial \mathbf{e} + \widehat{\mathbf{B}}^{\theta T} \partial \mathbf{k} + \widehat{\mathbf{C}}^{\theta T} \partial \mathbf{k}^\psi + \widehat{\mathbf{D}}^{\theta T} \partial \mathbf{w} + \widehat{\mathbf{E}}^\theta \partial \bar{\mathbf{q}}_z \\
 \mathbf{Q}^\phi &= \widehat{\mathbf{A}}^{\psi T} \partial \mathbf{e} + \widehat{\mathbf{B}}^{\psi T} \partial \mathbf{k} + \widehat{\mathbf{C}}^{\psi T} \partial \mathbf{k}^\psi + \widehat{\mathbf{D}}^{\psi T} \partial \mathbf{w} + \widehat{\mathbf{E}}^\psi \partial \bar{\mathbf{q}}_z
 \end{aligned} \tag{63}$$

Appendix D reports, for sake of brevity, the definition of the matrices of the constitutive relations, Eqs. (61)–(63), and the other matrices that appear in the governing equations, Eqs. (39)–(57), and in the boundary conditions, Eq. (58).

For simplicity, numerical examples are related to rectangular flat plates with the edges parallel to the axes (x_1, x_2). The length of the plate (in the x_1 direction) is denoted with a , and the width (in the x_2 direction) is denoted with b . The origin of the axes corresponds to the lower-left corner of the plate.

According to the plate dimensions (See Fig. 2), the previous boundary conditions used in this numerical analysis are the following ones:

- SS-1 → Simply supported symmetric cross-ply and sandwich plates

$$\begin{aligned}
 @x_1=0, a & \qquad \qquad \qquad e_{22} \quad e_{12} \\
 u_2 = w^{(0)} = w^{(1)} = w^{(2)} = \theta_2 = \psi_2 = e_{11} = k_{11} = k_{11}^\psi = 0 & \qquad \qquad \qquad = {}^{HR}E \\
 N_{11} + \frac{1}{\eta}(u_{1,1} - e_{11}) = M_{11} + \frac{1}{\eta}(\theta_{1,1} - k_{11}) = M_{11}^\phi + \frac{1}{\eta}(\psi_{1,1} - k_{11}^\psi) = {}^{HR}E & \qquad \qquad \qquad 1 \quad 1 \\
 = {}^{HR}K_1^{k22} = {}^{HR}K_1^{k12} = {}^{HR}K_1^{k22\psi} = {}^{HR}K_1^{k12\psi} = {}^{HR}K_1^{k21\psi} = 0 @x_2=0, b \quad u_1 = w^{(0)} = w^{(1)} & \qquad \qquad \qquad \\
 = w^{(2)} = \theta_1 = \psi_1 = e_{22} = k_{22} = k_{22}^\psi = 0 \quad N_{22} + \frac{1}{\eta}(u_{2,2} - e_{22}) = M_{22} + \frac{1}{\eta}(\theta_{2,2} - k_{22}) & \qquad \qquad \qquad \\
 = M_{22}^\phi + \frac{1}{\eta}(\psi_{2,2} - k_{22}^\psi) = {}^{HR}E_2^{e11} = {}^{HR}E_2^{e12} = {}^{HR}K_2^{k11} = {}^{HR}K_2^{k12} = {}^{HR}K_2^{k11\psi} = {}^{HR}K_2^{k12\psi} & \qquad \qquad \qquad \\
 = {}^{HR}K_2^{k21\psi} = 0 & \qquad \qquad \qquad
 \end{aligned} \tag{64}$$

- SS-2 → Simply supported antisymmetric angle-ply

$$\begin{aligned}
 @x_1 = 0, a & \qquad \qquad \qquad e_{11} \quad e_{22} \\
 u_1 = w^{(0)} = w^{(1)} = w^{(2)} = \theta_2 = \psi_2 = e_{12} = k_{11} = k_{11}^\psi = 0 & \qquad \qquad \qquad = {}^{HR}E \quad = {}^{HR}K_1^{k22} = {}^{HR}K_1^{k12} = {}^{HR}K_1^{k22\psi} = {}^{HR}K_1^{k12\psi} = {}^{HR}K_1^{k21\psi} = 0 @x_2 \\
 N_{12} + \frac{1}{\eta}(u_{1,2} + u_{2,1} - e_{12}) = M_{11} + \frac{1}{\eta}(\theta_{1,1} - k_{11}) = M_{11}^\phi + \frac{1}{\eta}(\psi_{1,1} - k_{11}^\psi) = {}^{HR}E & \qquad \qquad \qquad 1 \quad 1 \\
 = 0, b \quad u_2 = w^{(0)} = w^{(1)} = w^{(2)} = \theta_1 = \psi_1 = e_{12} = k_{22} = k_{22}^\psi = 0 \quad N_{12} + \frac{1}{\eta}(u_{1,2} + u_{2,1} - e_{12}) = M_{22} + \frac{1}{\eta}(\theta_{2,2} - k_{22}) = M_{22}^\phi + \frac{1}{\eta}(\psi_{2,2} - k_{22}^\psi) = {}^{HR}E_2^{e11} & \qquad \qquad \qquad \\
 = {}^{HR}E_2^{e22} = {}^{HR}K_2^{k11} = {}^{HR}K_2^{k12} = {}^{HR}K_2^{k11\psi} = {}^{HR}K_2^{k12\psi} = {}^{HR}K_2^{k21\psi} = 0 & \qquad \qquad \qquad
 \end{aligned} \tag{65}$$

Table 1
Material properties (all Young and shear moduli are expressed in MPa).

Material Name	E_1	E_2	E_3	ν_{12}	ν_{13}	ν_{23}	G_{12}	G_{13}	G_{23}
A	25	1	1	0.25	0.25	0.25	0.5	0.5	0.2
B	110,000	7857	7857	0.33	0.33	0.49	3292	3292	1292
C	40.3	40.3	40.3	0.3	0.3	0.3	12	12	12

Table 2
Laminated composite and sandwich plates (the layer-stacking sequence starts from the bottom surface).

Name	Materials	$h^{(k)}/h$	Lamina Orientation [deg]
L1	A/A/A	0.25/0.5/0.25	0/90/0
L2	A/A	0.5/0.5	-15/15
L3	A/A/A/A	0.25/0.25/0.25/0.25	-30/30/-30/30
S1	B/B/C/B/B	0.05/0.05/0.8/0.05/0.05	0/90/Core/90/0

3. Numerical analysis

In this Section, the en-RZT_{3,2}^(m) is used to study the elasto-static behaviour of multilayered thick plates.

In order to assess the accuracy of this newly developed mixed model, the results are compared with exact three-dimensional solution available in literature framework. More specifically, for multilayered cross-ply and sandwich plates, the solution obtained by Pagano [2] has been used as reference, whereas, for angle-ply lamination schemes in which the effect of shear coupling is typically present, the other solution developed by Pagano [3] for cylindrical bending has been used as reference.

By using the Navier’s method to obtain the solution, for cross-ply or orthotropic rectangular plates with simply supported boundary conditions (SS-1) under bi-sinusoidal transverse pressure, the equilibrium equations and the BCs can be satisfied by the following set of trigonometric functions:

Table 3
Percentage errors for maximum deflection and strains.

	η	1.00E-02	1.00E-03	1.00E-04	1.00E-05	1.00E-06	1.00E-07	1.00E-08	1.00E-09	1.00E-10
deflection	L1	3.941E-01	3.404E-02	3.893E-03	-3.151E-03	-4.242E-03	-4.402E-03	-4.422E-03	-4.424E-03	-4.424E-03
	L2	2.210E-01	2.118E-01	2.104E-01	2.103E-01	2.103E-01	2.103E-01	2.103E-01	2.103E-01	2.103E-01
strains	L1	1.55E+04	8.63E+03	1.83E+03	2.09E+02	2.12E+01	2.12E+00	2.12E-01	2.12E-02	2.12E-03
	L2	4.08E+01	4.63E+00	4.71E-01	4.72E-02	4.72E-03	4.72E-04	4.72E-05	4.72E-06	4.72E-07

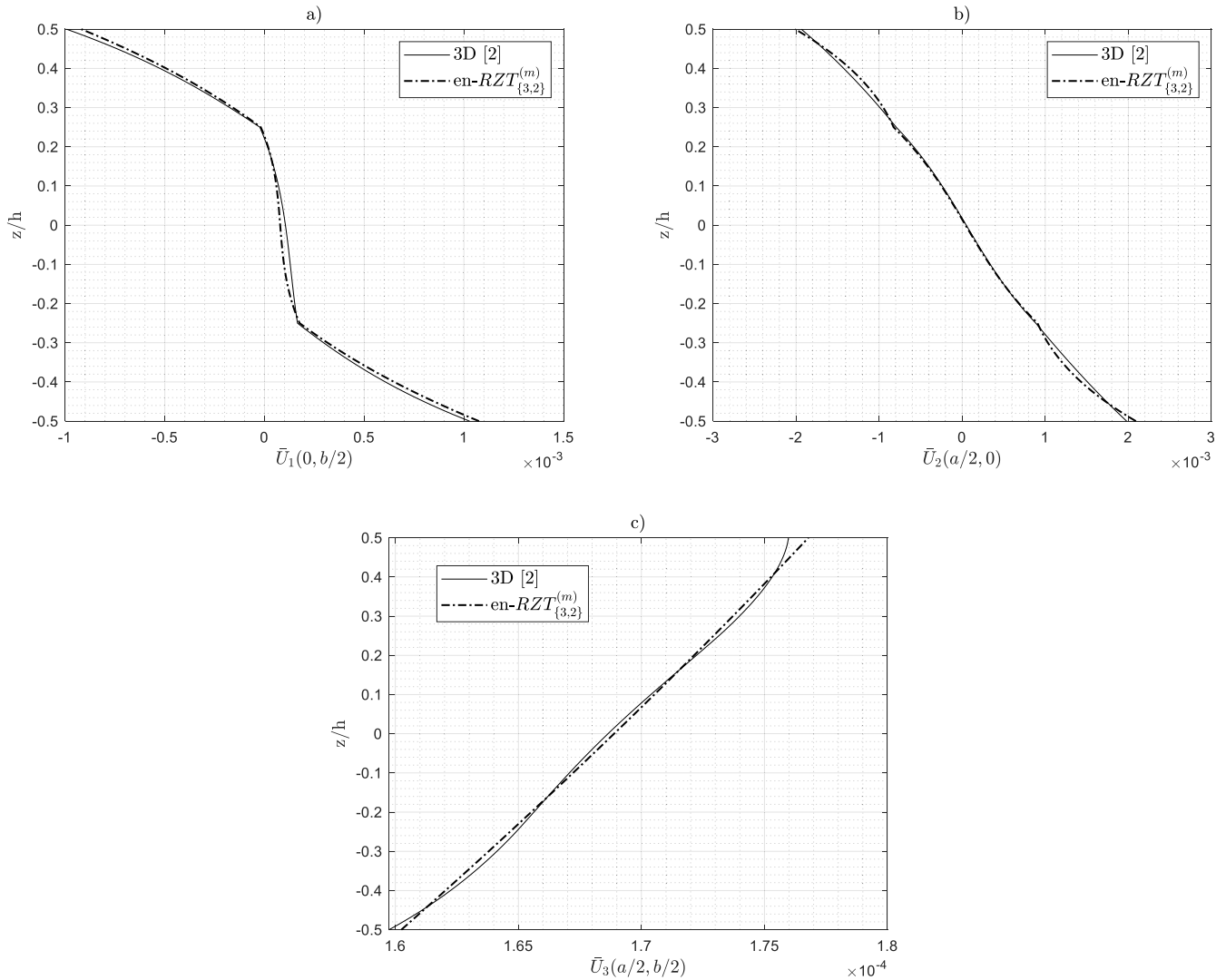


Fig. 3. Normalized through-the-thickness distributions for displacements and stresses in a simply supported (SS-1) square ($a/b = 1$) thick ($a/h = 4$) three-layered cross-ply under bi-sinusoidal pressure on top surface.

$$\begin{aligned}
 u_1(\mathbf{x}) &= U \cos(\lambda_m x_1) \sin(\lambda_n x_2); & u_2(\mathbf{x}) &= V \sin(\lambda_m x_1) \cos(\lambda_n x_2); \\
 w^{(0)}(\mathbf{x}) &= W^{(0)} \sin(\lambda_m x_1) \sin(\lambda_n x_2); & w^{(1)}(\mathbf{x}) &= W^{(1)} \sin(\lambda_m x_1) \sin(\lambda_n x_2); & w^{(2)}(\mathbf{x}) &= W^{(2)} \sin(\lambda_m x_1) \sin(\lambda_n x_2); \\
 \theta_1(\mathbf{x}) &= \Theta_1 \cos(\lambda_m x_1) \sin(\lambda_n x_2); & \theta_2(\mathbf{x}) &= \Theta_2 \sin(\lambda_m x_1) \cos(\lambda_n x_2); \\
 \psi_1(\mathbf{x}) &= \Psi_1 \cos(\lambda_m x_1) \sin(\lambda_n x_2); & \psi_2(\mathbf{x}) &= \Psi_2 \sin(\lambda_m x_1) \cos(\lambda_n x_2); \\
 e_{11}(\mathbf{x}) &= E_{11} \sin(\lambda_m x_1) \sin(\lambda_n x_2); & e_{22}(\mathbf{x}) &= E_{22} \sin(\lambda_m x_1) \sin(\lambda_n x_2); & e_{12}(\mathbf{x}) &= E_{12} \cos(\lambda_m x_1) \cos(\lambda_n x_2); \\
 k_{11}(\mathbf{x}) &= K_{11} \sin(\lambda_m x_1) \sin(\lambda_n x_2); & k_{22}(\mathbf{x}) &= K_{22} \sin(\lambda_m x_1) \sin(\lambda_n x_2); & k_{12}(\mathbf{x}) &= K_{12} \cos(\lambda_m x_1) \cos(\lambda_n x_2); \\
 k_{11}^w(\mathbf{x}) &= K_{11}^w \sin(\lambda_m x_1) \sin(\lambda_n x_2); & k_{22}^w(\mathbf{x}) &= K_{22}^w \sin(\lambda_m x_1) \sin(\lambda_n x_2); \\
 k_{12}^w(\mathbf{x}) &= K_{12}^w \cos(\lambda_m x_1) \cos(\lambda_n x_2); & k_{21}^w(\mathbf{x}) &= K_{21}^w \cos(\lambda_m x_1) \cos(\lambda_n x_2)
 \end{aligned} \tag{66}$$

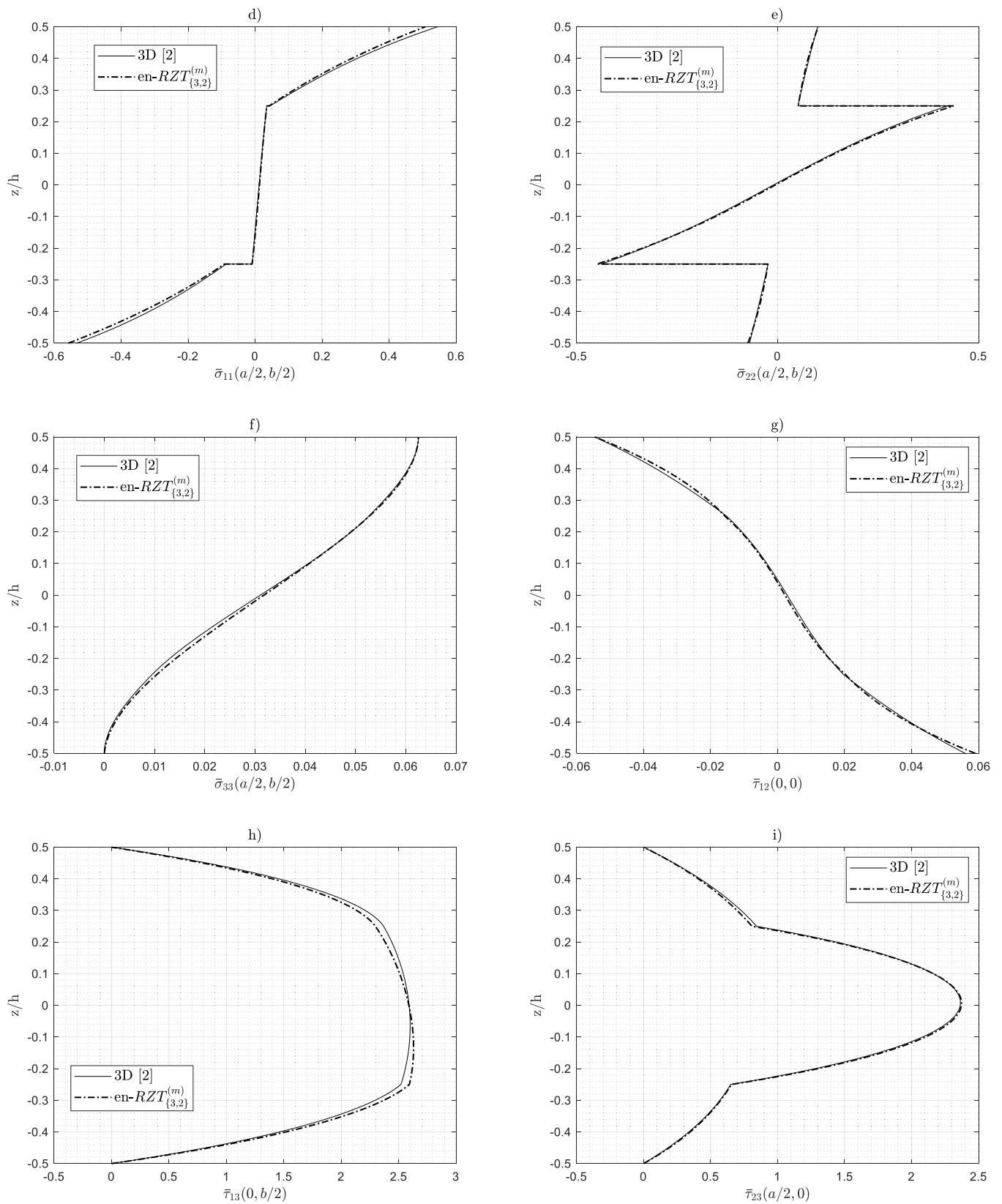


Fig. 3. (continued).

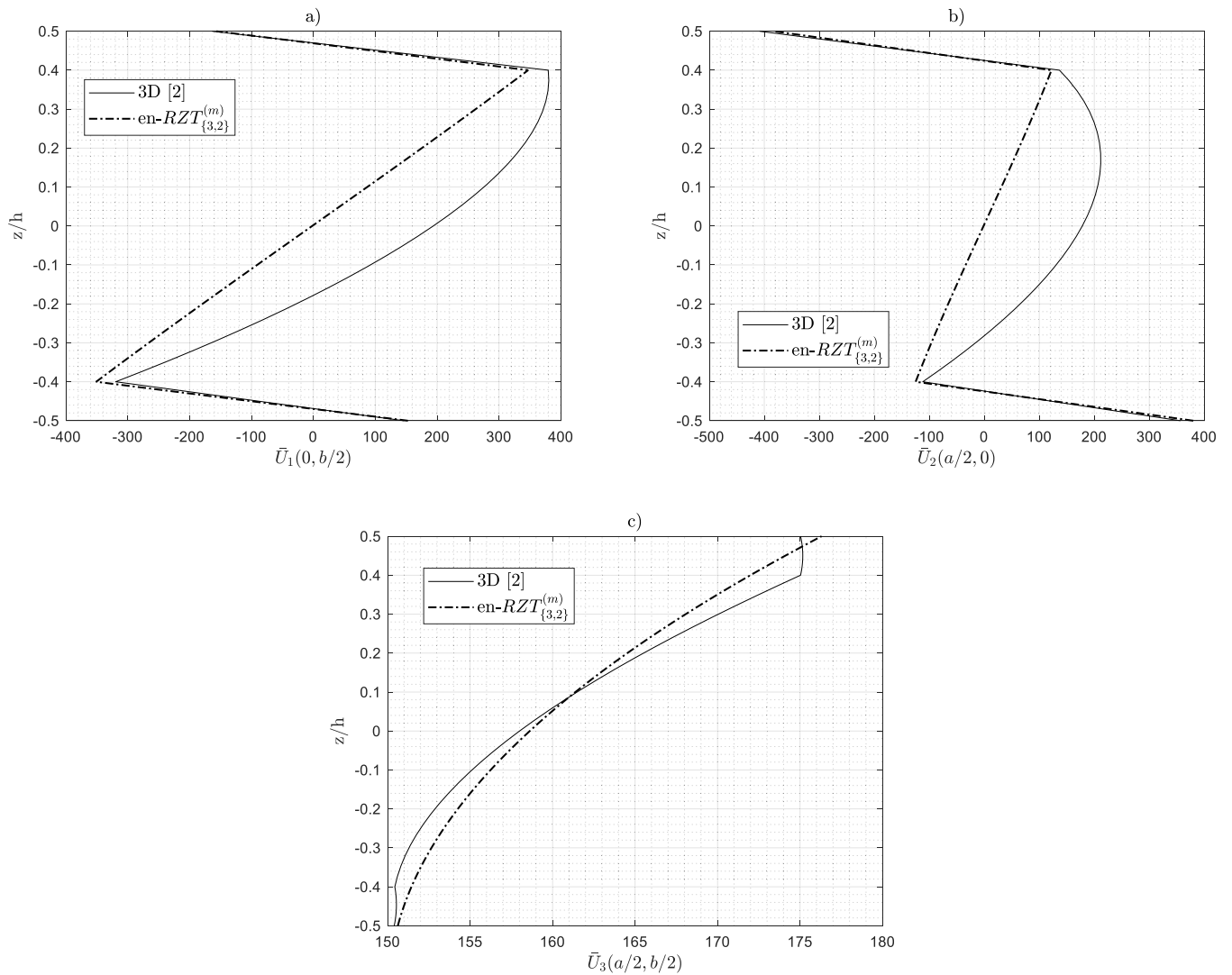


Fig. 4. Normalized through-the-thickness distributions for displacements and stresses in a simply supported (SS-1) square ($a/b = 1$) thick ($a/h = 4$) sandwich with cross-ply face-sheets and soft core, under bi-sinusoidal pressure on top surface.

where $\lambda_m = m\pi/a$; $\lambda_n = n\pi/b$ (m, n are half-wave number in x_1 and x_2 directions, respectively).

For antisymmetric angle-ply laminated plates simply supported on all edges, a solution for both the governing equations and the boundary conditions can be obtained by using the Navier's method with the following trigonometric functions (SS-2):

$$\begin{aligned}
 u_1(\mathbf{x}) &= U \sin(\lambda_m x_1) \cos(\lambda_n x_2); & u_2(\mathbf{x}) &= V \cos(\lambda_m x_1) \sin(\lambda_n x_2); \\
 w^{(0)}(\mathbf{x}) &= W^{(0)} \sin(\lambda_m x_1) \sin(\lambda_n x_2); & w^{(1)}(\mathbf{x}) &= W^{(1)} \sin(\lambda_m x_1) \sin(\lambda_n x_2); & w^{(2)}(\mathbf{x}) &= W^{(2)} \sin(\lambda_m x_1) \sin(\lambda_n x_2); \\
 \theta_1(\mathbf{x}) &= \Theta_1 \cos(\lambda_m x_1) \sin(\lambda_n x_2); & \theta_2(\mathbf{x}) &= \Theta_2 \sin(\lambda_m x_1) \cos(\lambda_n x_2); \\
 \psi_1(\mathbf{x}) &= \Psi_1 \cos(\lambda_m x_1) \sin(\lambda_n x_2); & \psi_2(\mathbf{x}) &= \Psi_2 \sin(\lambda_m x_1) \cos(\lambda_n x_2); \\
 e_{11}(\mathbf{x}) &= E_{11} \cos(\lambda_m x_1) \cos(\lambda_n x_2); & e_{22}(\mathbf{x}) &= E_{22} \cos(\lambda_m x_1) \cos(\lambda_n x_2); & e_{12}(\mathbf{x}) &= E_{12} \sin(\lambda_m x_1) \sin(\lambda_n x_2); \\
 k_{11}(\mathbf{x}) &= K_{11} \sin(\lambda_m x_1) \sin(\lambda_n x_2); & k_{22}(\mathbf{x}) &= K_{22} \sin(\lambda_m x_1) \sin(\lambda_n x_2); & k_{12}(\mathbf{x}) &= K_{12} \cos(\lambda_m x_1) \cos(\lambda_n x_2); \\
 k_{11}^w(\mathbf{x}) &= K_{11}^w \sin(\lambda_m x_1) \sin(\lambda_n x_2); & k_{22}^w(\mathbf{x}) &= K_{22}^w \sin(\lambda_m x_1) \sin(\lambda_n x_2); \\
 k_{12}^w(\mathbf{x}) &= K_{12}^w \cos(\lambda_m x_1) \cos(\lambda_n x_2); & k_{21}^w(\mathbf{x}) &= K_{21}^w \cos(\lambda_m x_1) \cos(\lambda_n x_2)
 \end{aligned}$$

(67)

Moreover, in the following examples, the in-plane prescribed tractions on top and bottom surfaces are null and only a transverse load pressure has been considered:

$$\begin{aligned}
 \bar{p}_{1(B)} &= 0 \\
 \bar{p}_{1(T)} &= 0 \\
 \bar{p}_{2(B)} &= 0 \\
 \bar{p}_{2(T)} &= 0
 \end{aligned}$$

(68)

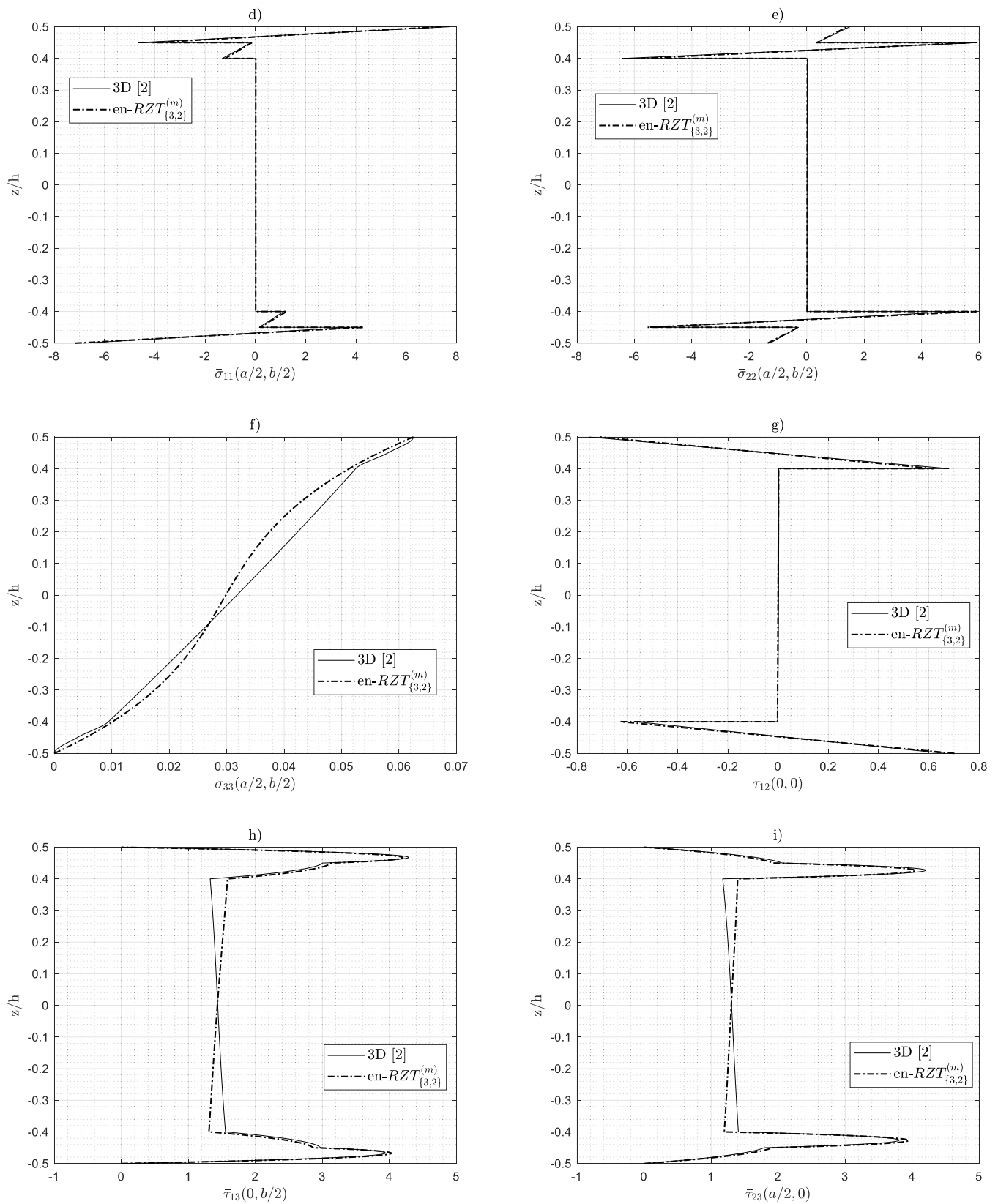


Fig. 4. (continued).

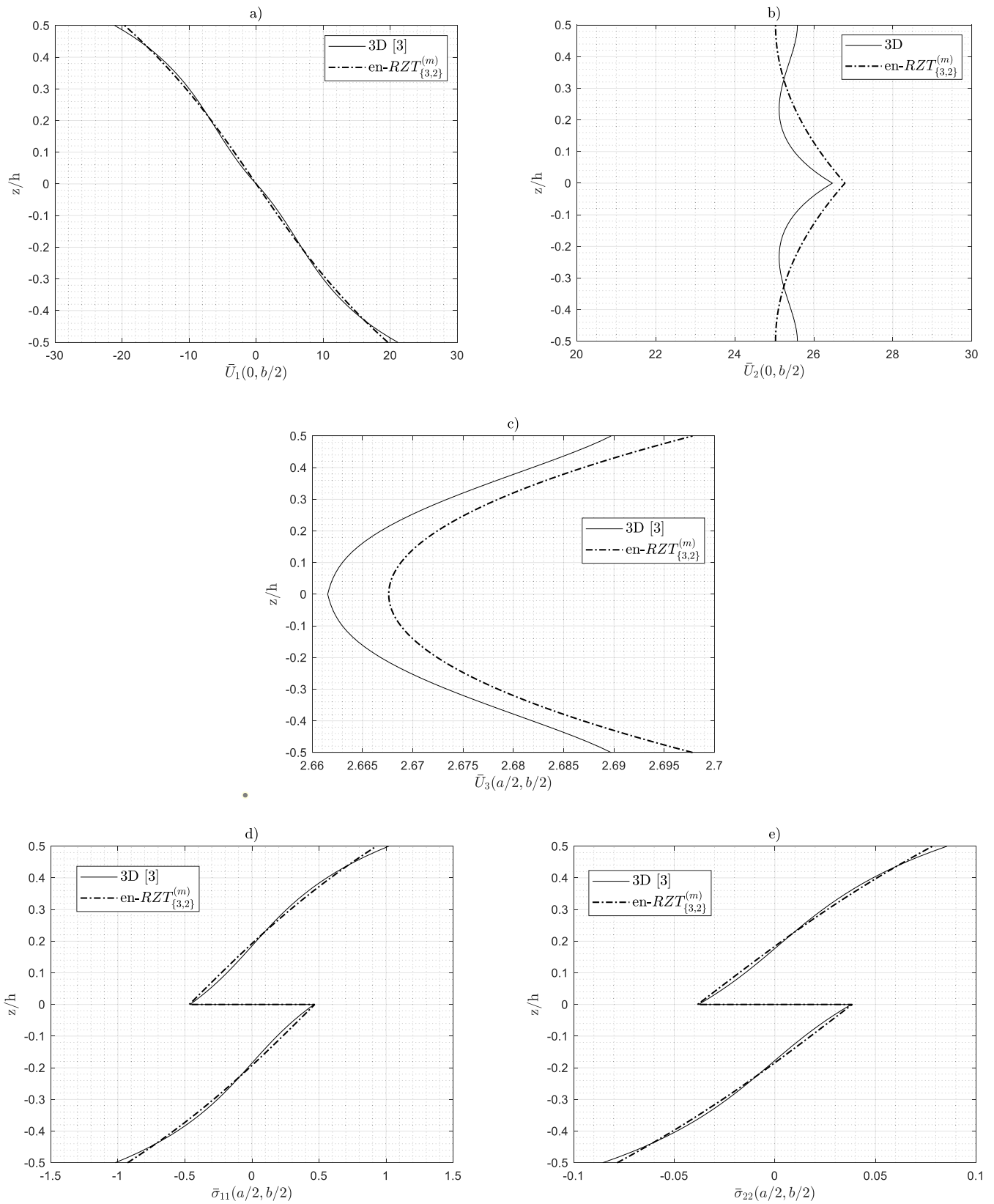


Fig. 5. Normalized through-the-thickness distributions for displacements and stresses in a simply supported (SS-2) thick ($a/h = 4$) antisymmetric two-layered angle ply $[-15/15]$ under bi-sinusoidal pressure acting on top and bottom surfaces.

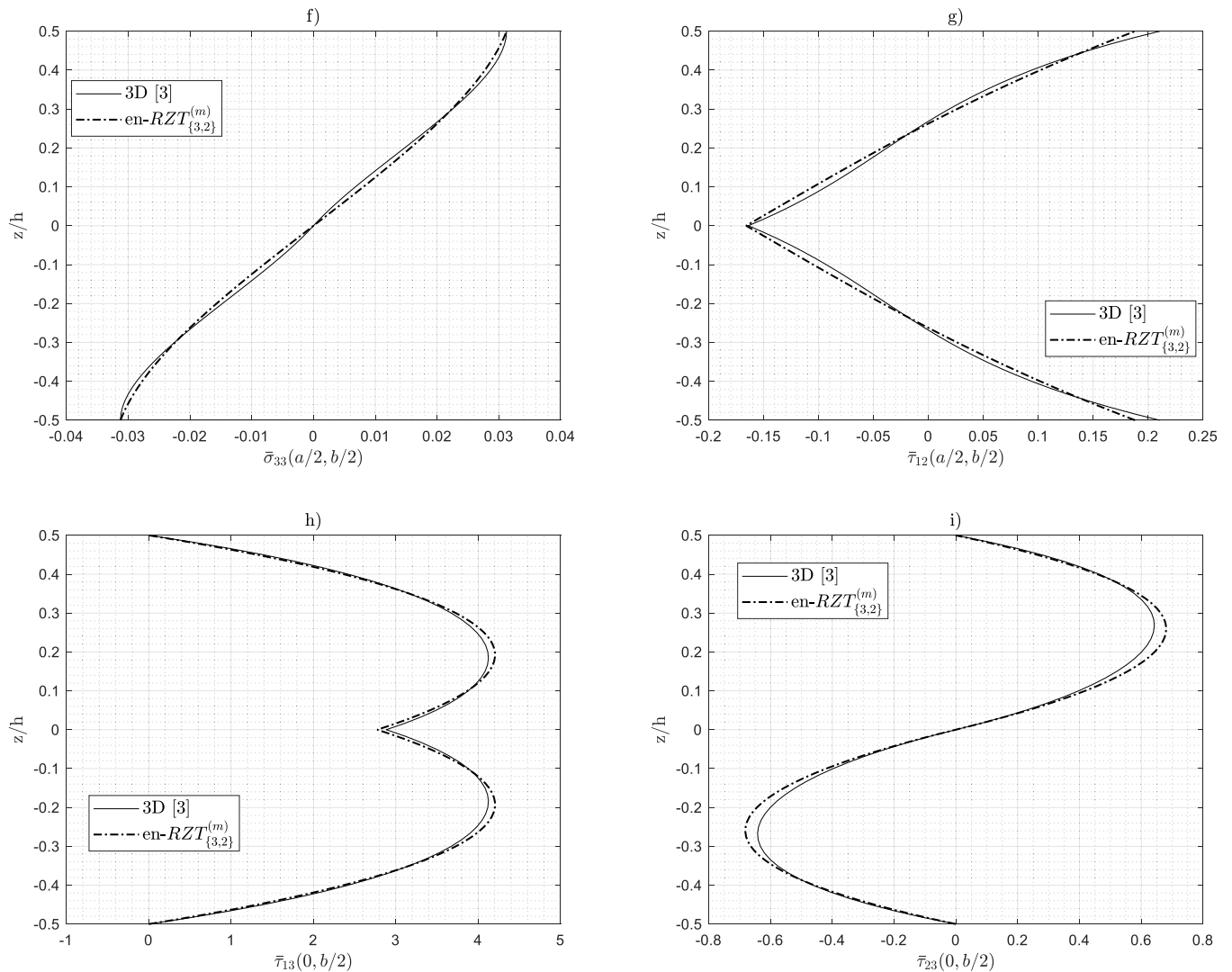


Fig. 5. (continued).

If not otherwise specified, the transverse applied load pressure has the following expression;

$$\begin{aligned} \bar{p}_{3(B)} &= \bar{q}_{3(B)} \sin(\lambda_m x_1) \sin(\lambda_n x_2) \\ \bar{p}_{3(T)} &= \bar{q}_{3(T)} \sin(\lambda_m x_1) \sin(\lambda_n x_2) \end{aligned} \quad (69)$$

where $\bar{q}_{3(B)}$ and $\bar{q}_{3(T)}$ are the maximum values.

The materials used in this analysis are defined in Table 1. Material A and B are orthotropic and material C is an isotropic polymeric soft foam.

Table 2 reports the layer stacking-sequences for the plates investigated in this numerical assessment.

The non-dimensional quantities, if not otherwise specified, are defined as follows:

$$\begin{aligned} \{\bar{U}_1, \bar{U}_2\} &= 1000 \frac{E_2 h^2}{\bar{p}_3 a_1^2} \{U_1, U_2\}; & \bar{U}_3 &= 100 \frac{E_2 h^3}{\bar{p}_3 a_1^3} U_3; \\ \{\bar{\sigma}_{11}, \bar{\sigma}_{22}, \bar{\sigma}_{33}, \bar{\tau}_{12}\} &= \frac{h^2 \{\sigma_{11}, \sigma_{22}, \sigma_{33}, \tau_{12}\}}{\bar{p}_3 a_1^2}; & \{\bar{\tau}_{13}, \bar{\tau}_{23}\} &= \frac{10h \{\tau_{13}, \tau_{23}\}}{\bar{p}_3 a_1}; \end{aligned} \quad (70)$$

Note that $\bar{p}_3 = \bar{q}_{3(B)} + \bar{q}_{3(T)}$, and for sandwich structures E_2 is considered the Young's modulus in the transverse direction of the face-sheet material.

3.1. Penalty parameter evaluation

By observing the equilibrium equations (see Eqs. (39)–(57)), it is clear that the accuracy of the results can be dependent on the value of the penalty parameter η related to the penalty functional for the enforcement of the compatibility between in-plane strain quantities. Generally, when the numerical value assumed by η in the penalty functional (see Eq. (34)) is low, that term in the variational statement has an important role to ensure the compatibility between the new strain variables and those derived from the kinematic field. Otherwise, if η assumes high values, the penalty term is less relevant and there can be discrepancies in the in-plane strain compatibilities. In order to evaluate the best range of η values that can guarantee a good accuracy of the results, a parametric investigation has been done. For the simply supported (SS-1) cross-ply laminate L1 and the simply supported (SS-2) anti-symmetric angle-ply L2, both under a bi-sinusoidal transverse pressure, the through-the-thickness averaged central deflections and the other strain quantities are computed using the Navier's method. According to Pagano [2,3] analytical three-dimensional solutions as reference results, Table 3 provide the percentage errors for the through-the-thickness averaged central deflections. Furthermore, for each value of the penalty parameter, the sum of the absolute errors in the strains compatibilities is evaluated for both plates. The errors on the deflection is decreasing with the decreasing of the penalty parameter value and

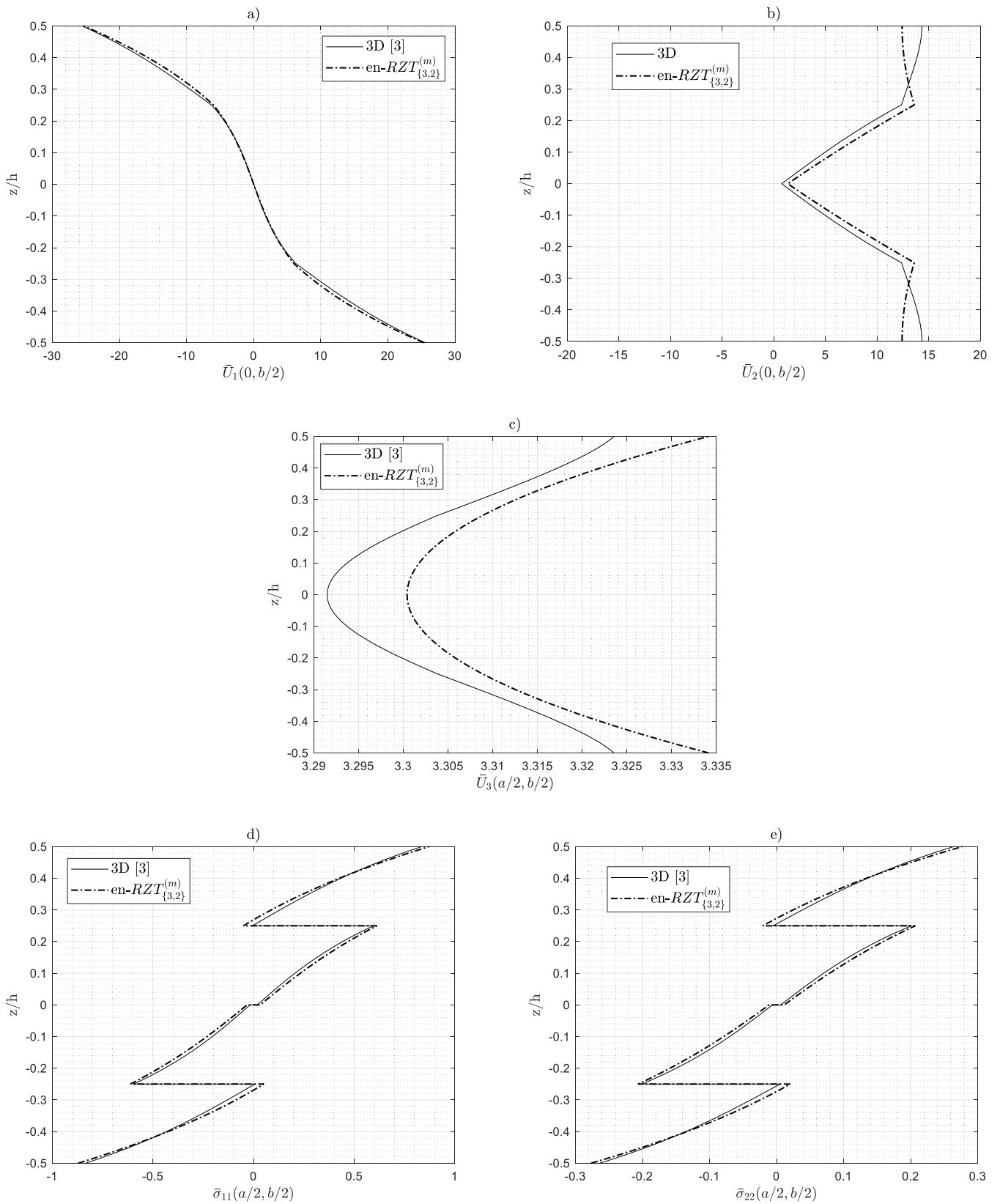


Fig. 6. Normalized through-the-thickness distributions for displacements and stresses in a simply supported (SS-2) thick ($a/h = 4$) antisymmetric four-layered angle-ply $[-30/30/-30/30]$ under bi-sinusoidal pressure acting on top and bottom surfaces.

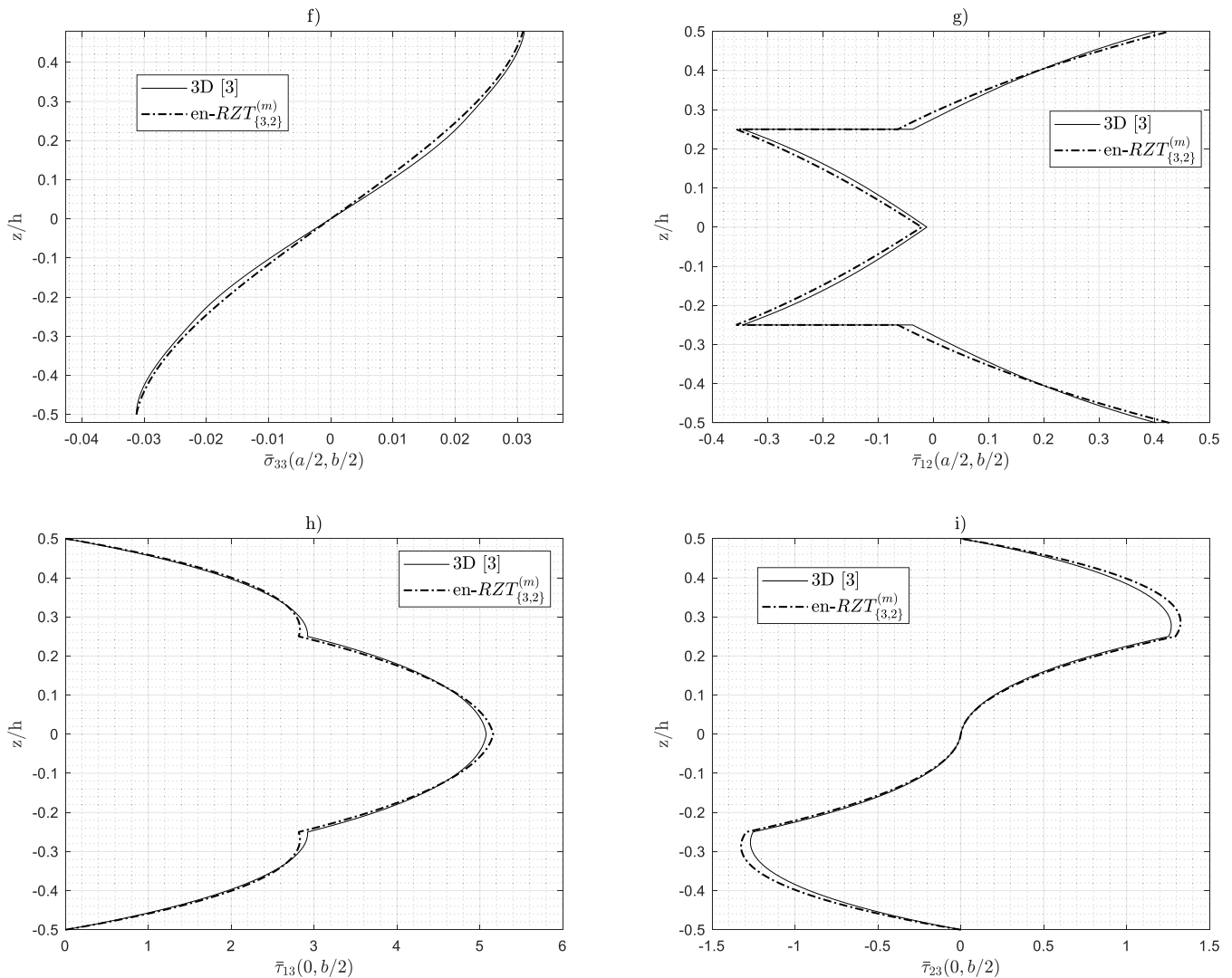


Fig. 6. (continued).

after $\eta = 10^{-5}$ is almost stable. As expected, the lower the value of the penalty parameter the better enforcement of the strain compatibility between the new strain variables and the strains obtained by the kinematic field.

Thus, the selected penalty parameter value for this numerical analysis is $\eta = 10^{-10}$, that is able to guarantee a good accuracy on the maximum displacement and a good compatibility on the strains quantities.

3.2. Cross-ply multilayered and sandwich plates

In this first numerical example, a three-layered cross-ply plate (L1) is considered. The squared ($a/b = 1$) plate is simply supported (SS-1) on all edges and the length to thickness ratio is here considered as $a/h = 4$.

In order to obtain a non-negligible transverse normal deformation, the transverse distributed load is applied on the top surface only, i.e., $\bar{q}_{3(B)} = 0$.

In Fig. 3 (a-i), the through-the-thickness distributions of the normalized quantities are shown for the simply-supported three-layered symmetric cross-ply.

It is clear from Figs. 3 a) and b) how the en-RZT_{3,2}^{(m)} is able to match the exact three-dimensional distributions for in-plane displacements. Moreover, the parabolic expansion for the transverse displacement assumed in the kinematic field can predict with good agreement the

exact result. As expected, the non-linear distributions for in-plane stresses obtained using the constitutive relation of the en-RZT_{3,2}^{(m)} are very close to the exact three-dimensional ones and the transverse normal stress. Moreover, the transverse shear stress distributions are in very good agreement with the three-dimensional solution.

The next example considers a multilayered thick sandwich plate with cross-ply face-sheets (S1) and simply-supported (SS-1) edges. The length-to-thickness ratio is $a/h = 4$ and $a/b = 1$, with a the ratio between the core's thickness and each face's thickness equal to $h_c/h_f = 8$. Like in the previous example, the bi-sinusoidal transverse load is applied only to the top surface of the sandwich plate.

Fig. 4 (a-i) shows the normalized through-the-thickness distributions of non-dimensional displacements and stresses for the simply-supported square multilayered sandwich plate.

As expected, in sandwich structures with a soft core, the effect of transverse normal deformability is more pronounced, affecting the through-the-thickness distribution of the transverse displacement and leading to more complex distributions of in-plane displacements and stresses. The assumed transverse normal stress is still able to follow the three-dimensional distribution. Also, the parabolic transverse displacement provided by the present model is very close to the exact one, but the in-plane displacements approximation is accurate only in the face-sheets. The higher-order zigzag functions are not able to represent the non-linear and non-symmetric distributions of displacements in the

core. On the other hand, the in-plane stresses are very close to the exact ones, especially at the layer interfaces. Also, the prediction of the transverse shear stresses is very accurate.

3.3. Antisymmetric angle-ply multilayered plates

In this Section, the family of angle-ply multilayered structures is investigated.

In this first example, a two-layered antisymmetric angle-ply plate (L2) is considered. The simply-supported conditions (SS-2) are considered here, and to use the Navier's solution and to compare the results with the exact analytical solution provided by Pagano [3] for the cylindrical bending assumptions, the length b (along the x_2 direction) is assumed to be much higher than the size along the x_1 direction ($b/a = 1000$). The length-to-thickness ratio here is $a/h = 4$, typical for a thick plate. As observed in the previous numerical examples, the transverse normal stretching effect is typical of sandwich structures, where the core has a very low stiffness with respect to the face-sheets. In fact, in the monolithic multilayered structures, the transverse normal deformability has an almost negligible effect on the laminate behaviour. For this reason, in the next examples, the bi-sinusoidal transverse pressure has been equally divided between the top and the bottom surfaces.

Fig. 5 (a-i) show the through-the-thickness normalized quantities for the antisymmetric two-layered angle-ply plate.

From Fig. 5, for through-the-thickness in-plane displacements and stresses, it is observed the same accuracy of the en-RZT(m){3,2} with respect to the three-dimensional solution. The novelty of this mixed model in the transverse shear stresses assumption can provide a remarkable accuracy in predicting these quantities. As observed in Figs. 5 h) and i), the percentage errors between the en-RZT(m){3,2} and the exact results for the peak values are 1.93% and 6.54% for τ_{13} and τ_{23} , respectively.

In order to assess the ability of the present mixed model to predict more complex transverse shear stress distributions for angle-ply multilayered structures, an anti-symmetric angle-ply laminate with more layers is considered (L3). Also for this case the simply supported condition (SS-2) and cylindrical bending assumption for the exact three-dimensional solution is considered to compare the numerical results with Pagano's solution [3]. Fig. 6 shows the results for normalized through-the-thickness quantities.

As expected, the en-RZT(m){3,2} is able to provide very accurate results for transverse shear stress distributions also with more complex lamination schemes. The higher-order zigzag functions are able to provide the non-linear through-the-thickness distribution for in-plane displacements and in-plane stresses. The parabolic transverse displacement, as well as all the transverse stress distributions, are in a very good agreement with the exact three-dimensional solution.

4. Conclusions

In this paper, a new mixed model has been developed based on the enhanced Refined Zigzag Theory and enhanced with cubic in-plane displacements and a parabolic transverse displacement. A new set of cubic zigzag functions have been obtained from the original kinematic

Appendix A

Derivation of the assumed transverse normal stress

In this appendix are given the details for the solution of the weak form of the compatibility constraint between the transverse normal strain derived from the kinematic field and that derived from the assumed transverse normal stress. This procedure described is similar to that developed by Iurlaro et al. [41] but here is recalled and used for a more general lamination scheme that involves the presence of the enhanced higher-order zigzag functions.

Due to the arbitrary variation of the unknown stress vector $\mathbf{q}_\sigma(\mathbf{x})$, the Eq. (36) can be solved as follows:

field, enforcing the transverse shear stress to vanish on the top and bottom external surfaces. This new mixed model, en-RZT(m){3,2}, has the transverse normal stress assumed a-priori as a through-the-thickness continuous cubic function and the transverse shear stresses assumed from the three-dimensional local equilibrium equations by involving an independent strain field. The Hellinger-Reissner functional has been used to enforce the compatibility of the transverse normal and shear strains between those coming from the independent field and those from the displacement one. Furthermore, a penalty term has been added to the governing functional in order to enforce the compatibility between the assumed strain variables used for the transverse shear stresses and the strains derived from the kinematic field.

The accuracy of the en-RZT(m){3,2} has been assessed by comparing its results with the exact three-dimensional solutions available in the literature for simply-supported thick multilayered and sandwich plates. The numerical investigation reveals the remarkable accuracy of the proposed model in computing the through-the-thickness distribution of displacements and in-plane stresses for cross-ply and angle-ply multilayered and sandwich structures. Moreover, the cubic terms in the in-plane displacements are able to represent the typical through-the-thickness nonlinear distributions for displacements and stresses.

The assumed transverse shear stresses with the combination of independent strain variables and the compatibility strain condition through the penalty functional can accurately predict a distribution very close to the three-dimensional elasticity one. Moreover, this model is able to predict the effect of shear coupling typically present in multilayered angle-ply plates. In fact, with respect to the procedure developed in the previous mixed RZT models, in the present one, all the derivatives of the kinematic variables introduced as new strain variables are considered, thus allowing to predict the transverse shear stress distributions accurately.

As a final consideration, it is possible to formulate efficient and computationally attractive finite elements with appropriate reduction methods, using the en-RZT(m){3,2}, since in the governing functional, it is required only the C^0 -continuity of all the unknowns (kinematic variables and strains variables for the transverse shear stresses).

CRediT authorship contribution statement

M. Sorrenti: Conceptualization, Methodology, Software, Validation, Visualization, Investigation, Writing - original draft, Writing - review & editing. **M. Gherlone:** Conceptualization, Methodology, Software, Validation, Visualization, Supervision, Writing - original draft, Writing - review & editing.

Declaration of Competing Interest

The authors declare that they have no known competing financial interests or personal relationships that could have appeared to influence the work reported in this paper.

Data availability

Data will be made available on request.

$$\int_V \delta \sigma_{zz}^a (\varepsilon_{zz} - \varepsilon_{zz}^a) dV = \left\langle \delta \sigma_{33}^a (\varepsilon_{33} - \varepsilon_{33}^a) \right\rangle = 0 \quad (\text{A.1})$$

where the symbol $\langle \dots \rangle$ denotes the integration over all the plate thickness.

Using the material constitutive relation for the transverse normal strain, see Eq. (6) and here reported for simplicity, it reads:

$$\varepsilon_{33}^a(\mathbf{x}, z) = S_{33}^{(k)} \sigma_{33}^a(\mathbf{x}, z) - \mathbf{R}^{(k)} \boldsymbol{\varepsilon}_p^{(k)}(\mathbf{x}, z) \quad (\text{A.2})$$

Where $\mathbf{R}^{(k)} = [R_{13}^{(k)} \quad R_{23}^{(k)} \quad R_{63}^{(k)}]$ is extrapolated by the constitutive relations Eq. (6).

Performing the virtual variation of the transverse normal stress and substituting the expression of Eq. (A.2) into Eq. (A.1), it follows:

$$\left\langle \delta \mathbf{q}_\sigma(\mathbf{x})^T \mathbf{P}_\sigma^T(z) \left(\mathbf{H}_{,3}^{\varepsilon}(\mathbf{x}) \mathbf{w}(\mathbf{x}) - S_{33}^{(k)} (\mathbf{L}(z) \bar{\mathbf{q}}_z(\mathbf{x}) + \mathbf{P}_\sigma(z) \mathbf{q}_\sigma(\mathbf{x}) - \mathbf{R}^{(k)} \boldsymbol{\varepsilon}_p^{(k)}(\mathbf{x}, z)) \right) \right\rangle = 0 \quad (\text{A.3})$$

Substituting the expression for in-plane strain quantities as defined by Eq. (11), it results into the following equation:

$$\left\langle \mathbf{P}_\sigma^T \mathbf{H}_{,3}^{\varepsilon} \right\rangle \mathbf{w} - \left\langle S_{33}^{(k)} \mathbf{P}_\sigma^T \mathbf{L} \right\rangle \bar{\mathbf{q}}_z - \left\langle S_{33}^{(k)} \mathbf{P}_\sigma^T \mathbf{P}_\sigma \right\rangle \mathbf{q}_\sigma + \left\langle \mathbf{P}_\sigma^T \mathbf{R}^{(k)} \right\rangle \boldsymbol{\varepsilon}_m + \left\langle \mathbf{P}_\sigma^T \mathbf{R}^{(k)} z \right\rangle \boldsymbol{\varepsilon}_\theta + \left\langle \mathbf{P}_\sigma^T \mathbf{R}^{(k)} \mathbf{M}^{(k)} \right\rangle \boldsymbol{\varepsilon}_\psi = 0 \quad (\text{A.4})$$

From which it is possible to solve in terms of the vector $\mathbf{q}_\sigma(\mathbf{x})$ that contains the unknown stress quantities:

$$\begin{aligned} \mathbf{q}_\sigma(\mathbf{x}) = & \left\langle S_{33}^{(k)} \mathbf{P}_\sigma^T \mathbf{P}_\sigma \right\rangle^{-1} \left\langle \mathbf{P}_\sigma^T \mathbf{H}_{,3}^{\varepsilon} \right\rangle \mathbf{w}(\mathbf{x}) - \left\langle S_{33}^{(k)} \mathbf{P}_\sigma^T \mathbf{P}_\sigma \right\rangle^{-1} \left\langle S_{33}^{(k)} \mathbf{P}_\sigma^T \mathbf{L} \right\rangle \bar{\mathbf{q}}_z(\mathbf{x}) + \left\langle S_{33}^{(k)} \mathbf{P}_\sigma^T \mathbf{P}_\sigma \right\rangle^{-1} \left\langle \mathbf{P}_\sigma^T \mathbf{R}^{(k)} \right\rangle \boldsymbol{\varepsilon}_m(\mathbf{x}) + \\ & + \left\langle S_{33}^{(k)} \mathbf{P}_\sigma^T \mathbf{P}_\sigma \right\rangle^{-1} \left\langle \mathbf{P}_\sigma^T \mathbf{R}^{(k)} z \right\rangle \boldsymbol{\varepsilon}_\theta(\mathbf{x}) + \left\langle S_{33}^{(k)} \mathbf{P}_\sigma^T \mathbf{P}_\sigma \right\rangle^{-1} \left\langle \mathbf{P}_\sigma^T \mathbf{R}^{(k)} \mathbf{M}^{(k)} \right\rangle \boldsymbol{\varepsilon}_\psi(\mathbf{x}) \end{aligned} \quad (\text{A.5})$$

The substituting the expression (A.5) into (26) after some mathematics, it is possible to write the final expression:

$$\sigma_{33}^a(\mathbf{x}, z) = \mathbf{A}_\sigma^u(z) \boldsymbol{\varepsilon}_m(\mathbf{x}) + \mathbf{A}_\sigma^\theta(z) \boldsymbol{\varepsilon}_\theta(\mathbf{x}) + \mathbf{A}_\sigma^\psi(z) \boldsymbol{\varepsilon}_\psi(\mathbf{x}) + \mathbf{A}_\sigma^w(z) \mathbf{w}(\mathbf{x}) + \mathbf{A}_\sigma^{qz}(z) \bar{\mathbf{q}}_z(\mathbf{x}) \quad (\text{A.6})$$

where

$$\begin{aligned} \mathbf{A}_\sigma^u(z) &= \mathbf{P}_\sigma(z) \left\langle S_{33}^{(k)} \mathbf{P}_\sigma(z)^T \mathbf{P}_\sigma(z) \right\rangle^{-1} \left\langle \mathbf{P}_\sigma(z)^T \mathbf{R}^{(k)} \right\rangle; \\ \mathbf{A}_\sigma^\theta(z) &= \mathbf{P}_\sigma(z) \left\langle S_{33}^{(k)} \mathbf{P}_\sigma(z)^T \mathbf{P}_\sigma(z) \right\rangle^{-1} \left\langle \mathbf{P}_\sigma(z)^T \mathbf{R}^{(k)} z \right\rangle; \\ \mathbf{A}_\sigma^\psi(z) &= \mathbf{P}_\sigma(z) \left\langle S_{33}^{(k)} \mathbf{P}_\sigma(z)^T \mathbf{P}_\sigma(z) \right\rangle^{-1} \left\langle \mathbf{P}_\sigma(z)^T \mathbf{R}^{(k)} \mathbf{M}^{(k)}(z) \right\rangle; \\ \mathbf{A}_\sigma^w(z) &= \mathbf{P}_\sigma(z) \left\langle S_{33}^{(k)} \mathbf{P}_\sigma(z)^T \mathbf{P}_\sigma(z) \right\rangle^{-1} \left\langle \mathbf{P}_\sigma(z)^T \mathbf{H}_{,3}^{\varepsilon} \right\rangle; \\ \mathbf{A}_\sigma^{qz}(z) &= \left[\mathbf{L}(z) - \mathbf{P}_\sigma(z) \left\langle S_{33}^{(k)} \mathbf{P}_\sigma(z)^T \mathbf{P}_\sigma(z) \right\rangle^{-1} \left\langle S_{33}^{(k)} \mathbf{P}_\sigma(z)^T \mathbf{L}(z) \right\rangle \right] \end{aligned} \quad (\text{A.7})$$

are the shape functions of the thickness coordinate for the transverse normal stress.

Appendix B

Derivation of the assumed transverse shear stresses

In this appendix is reported in details the formulation of the transverse shear stresses by performing the integration of the local equilibrium equations.

Using the assumed transverse normal stress expression defined by Eq. (38) and substituting into the material constitutive relations (see, Eq. (6)), the in-plane stress quantities are here defined in a compact matrix form:

$$\begin{aligned} \left\{ \begin{array}{l} \sigma_{11}^{(k)}(\mathbf{x}, z) \\ \sigma_{22}^{(k)}(\mathbf{x}, z) \\ \tau_{12}^{(k)}(\mathbf{x}, z) \end{array} \right\} &= \boldsymbol{\sigma}_p^{(k)} = \mathbf{Q}_p^{(k)} \boldsymbol{\varepsilon}_p^{(k)}(\mathbf{x}, z) + \mathbf{R}^{(k)} \sigma_{33}^a(\mathbf{x}, z) = \\ &= \mathbf{Q}_p^{(k)} \boldsymbol{\varepsilon}_m(\mathbf{x}) + z \mathbf{Q}_p^{(k)} \boldsymbol{\varepsilon}_\theta(\mathbf{x}) + \mathbf{Q}_p^{(k)} \mathbf{M}^{(k)} \boldsymbol{\varepsilon}_\psi(\mathbf{x}) + \\ &+ \mathbf{R}^{(k)} (\mathbf{A}_\sigma^u(z) \boldsymbol{\varepsilon}_m(\mathbf{x}) + \mathbf{A}_\sigma^\theta(z) \boldsymbol{\varepsilon}_\theta(\mathbf{x}) + \mathbf{A}_\sigma^\psi(z) \boldsymbol{\varepsilon}_\psi(\mathbf{x}) + \mathbf{A}_\sigma^w(z) \mathbf{w}(\mathbf{x}) + \mathbf{A}_\sigma^{qz}(z) \bar{\mathbf{q}}_z(\mathbf{x})) = \\ &= (\mathbf{Q}_p^{(k)} + \mathbf{R}^{(k)} \mathbf{A}_\sigma^u(z)) \boldsymbol{\varepsilon}_m(\mathbf{x}) + (z \mathbf{Q}_p^{(k)} + \mathbf{R}^{(k)} \mathbf{A}_\sigma^\theta(z)) \boldsymbol{\varepsilon}_\theta(\mathbf{x}) + \\ &+ (\mathbf{Q}_p^{(k)} \mathbf{M}^{(k)} + \mathbf{R}^{(k)} \mathbf{A}_\sigma^\psi(z)) \boldsymbol{\varepsilon}_\psi(\mathbf{x}) + \mathbf{R}^{(k)} \mathbf{A}_\sigma^w(z) \mathbf{w}(\mathbf{x}) + \mathbf{R}^{(k)} \mathbf{A}_\sigma^{qz}(z) \bar{\mathbf{q}}_z(\mathbf{x}) \end{aligned} \quad (\text{B.1})$$

Before substituting into the expression of local equilibrium equations defined by Eq. (28), it will be performed the substitution of the strain quantities with the new set of independent variables as defined by Eq. (29). This procedure results in:

$$\begin{aligned} \boldsymbol{\sigma}_p^{(k)} &= (\mathbf{Q}_p^{(k)} + \mathbf{R}^{(k)} \mathbf{A}_\sigma^u(z)) \mathbf{e}(\mathbf{x}) + (z \mathbf{Q}_p^{(k)} + \mathbf{R}^{(k)} \mathbf{A}_\sigma^\theta(z)) \mathbf{k}(\mathbf{x}) + \\ &+ (\mathbf{Q}_p^{(k)} \mathbf{M}^{(k)} + \mathbf{R}^{(k)} \mathbf{A}_\sigma^\psi(z)) \mathbf{k}^w(\mathbf{x}) + \mathbf{R}^{(k)} \mathbf{A}_\sigma^w(z) \mathbf{w}(\mathbf{x}) + \mathbf{R}^{(k)} \mathbf{A}_\sigma^{qz}(z) \bar{\mathbf{q}}_z(\mathbf{x}) \end{aligned} \quad (\text{B.2})$$

Deriving the expression of Eq. (B.2) with respect to x_1 and x_2 directions and substituting into Eq. (28) the integration along the thickness direction is performed, resulting into the following expression:

$$\boldsymbol{\tau}_i^{\alpha}(\mathbf{x}, z) = -\bar{\mathbf{p}}^{(B)}(\mathbf{x}) + \mathbf{A}^z(z)\partial\mathbf{e}(\mathbf{x}) + \mathbf{B}^z(z)\partial\mathbf{k}(\mathbf{x}) + \mathbf{D}^z(z)\partial\mathbf{k}^{\psi}(\mathbf{x}) + \mathbf{E}^z(z)\partial\mathbf{w}(\mathbf{x}) + \mathbf{F}^z(z)\partial\bar{\mathbf{q}}_z(\mathbf{x}) \tag{B.3}$$

where $\mathbf{A}^z(z)$, $\mathbf{B}^z(z)$, $\mathbf{D}^z(z)$, $\mathbf{E}^z(z)$, $\mathbf{F}^z(z)$ are the shape functions in the transverse direction, and the derivative of the independent strain variables are defined as follows:

$$\begin{aligned} \partial\mathbf{e}(\mathbf{x})^T &= [e_{11,1} \quad e_{22,1} \quad e_{12,1} \quad e_{11,2} \quad e_{22,2} \quad e_{12,2}]; \\ \partial\mathbf{k}(\mathbf{x})^T &= [k_{11,1} \quad k_{22,1} \quad k_{12,1} \quad k_{11,2} \quad k_{22,2} \quad k_{12,2}]; \\ \partial\mathbf{k}^{\psi}(\mathbf{x})^T &= [k_{11,1}^{\psi} \quad k_{22,1}^{\psi} \quad k_{12,1}^{\psi} \quad k_{21,1}^{\psi} \quad k_{11,2}^{\psi} \quad k_{22,2}^{\psi} \quad k_{12,2}^{\psi} \quad k_{21,2}^{\psi}]; \\ \partial\mathbf{w}(\mathbf{x})^T &= [w_{,1}^{(0)} \quad w_{,1}^{(1)} \quad w_{,2}^{(0)} \quad w_{,2}^{(1)} \quad w_{,2}^{(2)}]; \\ \partial\bar{\mathbf{q}}_z(\mathbf{x})^T &= [\bar{p}_{3(B),1} \quad \bar{p}_{3(T),1} \quad \bar{p}_{3(B),2} \quad \bar{p}_{3(T),2}] \end{aligned} \tag{B.4}$$

The shape functions are expressed as follows:

$$\mathbf{A}^z(z) = \begin{bmatrix} -\left[\int_{-h/2}^z (Q_{11}^{(k)} + R_{13}^{(k)} A_{\sigma 11}^{\mu}) dz\right] & -\left[\int_{-h/2}^z (Q_{12}^{(k)} + R_{13}^{(k)} A_{\sigma 12}^{\mu}) dz\right] & -\left[\int_{-h/2}^z (Q_{16}^{(k)} + R_{13}^{(k)} A_{\sigma 13}^{\mu}) dz\right] & -\left[\int_{-h/2}^z (Q_{16}^{(k)} + R_{63}^{(k)} A_{\sigma 11}^{\mu}) dz\right] & -\left[\int_{-h/2}^z (Q_{26}^{(k)} + R_{63}^{(k)} A_{\sigma 12}^{\mu}) dz\right] & -\left[\int_{-h/2}^z (Q_{66}^{(k)} + R_{63}^{(k)} A_{\sigma 13}^{\mu}) dz\right] \\ -\left[\int_{-h/2}^z (Q_{16}^{(k)} + R_{63}^{(k)} A_{\sigma 11}^{\mu}) dz\right] & -\left[\int_{-h/2}^z (Q_{26}^{(k)} + R_{63}^{(k)} A_{\sigma 12}^{\mu}) dz\right] & -\left[\int_{-h/2}^z (Q_{66}^{(k)} + R_{63}^{(k)} A_{\sigma 13}^{\mu}) dz\right] & -\left[\int_{-h/2}^z (Q_{12}^{(k)} + R_{23}^{(k)} A_{\sigma 11}^{\mu}) dz\right] & -\left[\int_{-h/2}^z (Q_{22}^{(k)} + R_{23}^{(k)} A_{\sigma 12}^{\mu}) dz\right] & -\left[\int_{-h/2}^z (Q_{26}^{(k)} + R_{23}^{(k)} A_{\sigma 13}^{\mu}) dz\right] \end{bmatrix} \tag{B.5}$$

$$\mathbf{B}^z(z) = \begin{bmatrix} -\left[\int_{-h/2}^z (zQ_{11}^{(k)} + R_{13}^{(k)} A_{\sigma 11}^{\mu}) dz\right] & -\left[\int_{-h/2}^z (zQ_{12}^{(k)} + R_{13}^{(k)} A_{\sigma 12}^{\mu}) dz\right] & -\left[\int_{-h/2}^z (zQ_{16}^{(k)} + R_{13}^{(k)} A_{\sigma 13}^{\mu}) dz\right] & -\left[\int_{-h/2}^z (zQ_{16}^{(k)} + R_{63}^{(k)} A_{\sigma 11}^{\mu}) dz\right] & -\left[\int_{-h/2}^z (zQ_{26}^{(k)} + R_{63}^{(k)} A_{\sigma 12}^{\mu}) dz\right] & -\left[\int_{-h/2}^z (zQ_{66}^{(k)} + R_{63}^{(k)} A_{\sigma 13}^{\mu}) dz\right] \\ -\left[\int_{-h/2}^z (zQ_{16}^{(k)} + R_{63}^{(k)} A_{\sigma 11}^{\mu}) dz\right] & -\left[\int_{-h/2}^z (zQ_{26}^{(k)} + R_{63}^{(k)} A_{\sigma 12}^{\mu}) dz\right] & -\left[\int_{-h/2}^z (zQ_{66}^{(k)} + R_{63}^{(k)} A_{\sigma 13}^{\mu}) dz\right] & -\left[\int_{-h/2}^z (zQ_{12}^{(k)} + R_{23}^{(k)} A_{\sigma 11}^{\mu}) dz\right] & -\left[\int_{-h/2}^z (zQ_{22}^{(k)} + R_{23}^{(k)} A_{\sigma 12}^{\mu}) dz\right] & -\left[\int_{-h/2}^z (zQ_{26}^{(k)} + R_{23}^{(k)} A_{\sigma 13}^{\mu}) dz\right] \end{bmatrix} \tag{B.6}$$

$$\mathbf{D}^z(z) = \begin{bmatrix} -\left[\int_{-h/2}^z (Q_{11}^{(k)} \mu_{11}^{(k)} + Q_{66}^{(k)} \mu_{22}^{(k)} + R_{13}^{(k)} A_{\sigma 11}^{\mu}) dz\right] & -\left[\int_{-h/2}^z (Q_{12}^{(k)} \mu_{21}^{(k)} + Q_{66}^{(k)} \mu_{12}^{(k)} + R_{13}^{(k)} A_{\sigma 12}^{\mu}) dz\right] & -\left[\int_{-h/2}^z (Q_{16}^{(k)} \mu_{31}^{(k)} + Q_{66}^{(k)} \mu_{13}^{(k)} + R_{13}^{(k)} A_{\sigma 13}^{\mu}) dz\right] & -\left[\int_{-h/2}^z (Q_{11}^{(k)} \mu_{12}^{(k)} + Q_{66}^{(k)} \mu_{21}^{(k)} + R_{13}^{(k)} A_{\sigma 14}^{\mu}) dz\right] \\ -\left[\int_{-h/2}^z (Q_{16}^{(k)} \mu_{31}^{(k)} + Q_{66}^{(k)} \mu_{13}^{(k)} + R_{13}^{(k)} A_{\sigma 13}^{\mu}) dz\right] & -\left[\int_{-h/2}^z (Q_{28}^{(k)} \mu_{21}^{(k)} + C_{66}^{(k)} \mu_{12}^{(k)} + R_{63}^{(k)} A_{\sigma 12}^{\mu}) dz\right] & -\left[\int_{-h/2}^z (Q_{26}^{(k)} \mu_{31}^{(k)} + Q_{66}^{(k)} \mu_{13}^{(k)} + R_{63}^{(k)} A_{\sigma 13}^{\mu}) dz\right] & -\left[\int_{-h/2}^z (Q_{16}^{(k)} \mu_{12}^{(k)} + Q_{66}^{(k)} \mu_{21}^{(k)} + R_{63}^{(k)} A_{\sigma 14}^{\mu}) dz\right] \\ -\left[\int_{-h/2}^z (Q_{66}^{(k)} \mu_{11}^{(k)} + Q_{66}^{(k)} \mu_{22}^{(k)} + R_{63}^{(k)} A_{\sigma 11}^{\mu}) dz\right] & -\left[\int_{-h/2}^z (Q_{66}^{(k)} \mu_{21}^{(k)} + Q_{66}^{(k)} \mu_{12}^{(k)} + R_{63}^{(k)} A_{\sigma 12}^{\mu}) dz\right] & -\left[\int_{-h/2}^z (Q_{66}^{(k)} \mu_{31}^{(k)} + Q_{66}^{(k)} \mu_{13}^{(k)} + R_{63}^{(k)} A_{\sigma 13}^{\mu}) dz\right] & -\left[\int_{-h/2}^z (Q_{66}^{(k)} \mu_{12}^{(k)} + Q_{66}^{(k)} \mu_{21}^{(k)} + R_{63}^{(k)} A_{\sigma 14}^{\mu}) dz\right] \\ -\left[\int_{-h/2}^z (Q_{12}^{(k)} \mu_{21}^{(k)} + Q_{66}^{(k)} \mu_{12}^{(k)} + R_{23}^{(k)} A_{\sigma 11}^{\mu}) dz\right] & -\left[\int_{-h/2}^z (Q_{22}^{(k)} \mu_{21}^{(k)} + Q_{66}^{(k)} \mu_{12}^{(k)} + R_{23}^{(k)} A_{\sigma 12}^{\mu}) dz\right] & -\left[\int_{-h/2}^z (Q_{22}^{(k)} \mu_{31}^{(k)} + Q_{66}^{(k)} \mu_{13}^{(k)} + R_{23}^{(k)} A_{\sigma 13}^{\mu}) dz\right] & -\left[\int_{-h/2}^z (Q_{12}^{(k)} \mu_{12}^{(k)} + Q_{66}^{(k)} \mu_{21}^{(k)} + R_{23}^{(k)} A_{\sigma 14}^{\mu}) dz\right] \end{bmatrix} \tag{B.7}$$

$$\mathbf{E}^z(z) = \begin{bmatrix} -\left[\int_{-h/2}^z R_{13}^{(k)} A_{\sigma 11}^w dz\right] & -\left[\int_{-h/2}^z R_{13}^{(k)} A_{\sigma 12}^w dz\right] & -\left[\int_{-h/2}^z R_{13}^{(k)} A_{\sigma 13}^w dz\right] & -\left[\int_{-h/2}^z R_{63}^{(k)} A_{\sigma 11}^w dz\right] & -\left[\int_{-h/2}^z R_{63}^{(k)} A_{\sigma 12}^w dz\right] & -\left[\int_{-h/2}^z R_{63}^{(k)} A_{\sigma 13}^w dz\right] \\ -\left[\int_{-h/2}^z R_{63}^{(k)} A_{\sigma 11}^w dz\right] & -\left[\int_{-h/2}^z R_{63}^{(k)} A_{\sigma 12}^w dz\right] & -\left[\int_{-h/2}^z R_{63}^{(k)} A_{\sigma 13}^w dz\right] & -\left[\int_{-h/2}^z R_{23}^{(k)} A_{\sigma 11}^w dz\right] & -\left[\int_{-h/2}^z R_{23}^{(k)} A_{\sigma 12}^w dz\right] & -\left[\int_{-h/2}^z R_{23}^{(k)} A_{\sigma 13}^w dz\right] \end{bmatrix} \tag{B.8}$$

$$\mathbf{F}^z(z) = \begin{bmatrix} -\left[\int_{-h/2}^z R_{13}^{(k)} A_{\sigma 11}^{qz} dz\right] & -\left[\int_{-h/2}^z R_{13}^{(k)} A_{\sigma 12}^{qz} dz\right] & -\left[\int_{-h/2}^z R_{63}^{(k)} A_{\sigma 11}^{qz} dz\right] & -\left[\int_{-h/2}^z R_{63}^{(k)} A_{\sigma 12}^{qz} dz\right] \\ -\left[\int_{-h/2}^z R_{63}^{(k)} A_{\sigma 11}^{qz} dz\right] & -\left[\int_{-h/2}^z R_{63}^{(k)} A_{\sigma 12}^{qz} dz\right] & -\left[\int_{-h/2}^z R_{23}^{(k)} A_{\sigma 11}^{qz} dz\right] & -\left[\int_{-h/2}^z R_{23}^{(k)} A_{\sigma 12}^{qz} dz\right] \end{bmatrix} \tag{B.9}$$

Since the expression (B.3) is not able to satisfy the traction condition at the top surface, a further term is added:

$$\boldsymbol{\tau}_i^{\alpha}(\mathbf{x}, z) = -\bar{\mathbf{p}}^{(B)}(\mathbf{x}) + \mathbf{A}^z(z)\partial\mathbf{e}(\mathbf{x}) + \mathbf{B}^z(z)\partial\mathbf{k}(\mathbf{x}) + \mathbf{D}^z(z)\partial\mathbf{k}^{\psi}(\mathbf{x}) + \mathbf{E}^z(z)\partial\mathbf{w}(\mathbf{x}) + \mathbf{F}^z(z)\partial\bar{\mathbf{q}}_z(\mathbf{x}) + \mathbf{a}(z + h/2) \tag{B.10}$$

Performing the integration along the entire thickness, it is possible to compute the expression of \mathbf{a} as follows:

$$\mathbf{a} = -\frac{1}{h}(\bar{\mathbf{p}}^{(T)} + \bar{\mathbf{p}}^{(B)}) - \frac{1}{h}\langle \mathbf{A}^z \rangle \partial\mathbf{e} - \frac{1}{h}\langle \mathbf{B}^z \rangle \partial\mathbf{k} - \frac{1}{h}\langle \mathbf{D}^z \rangle \partial\mathbf{k}^{\psi} + \frac{1}{h}\langle \mathbf{E}^z \rangle \partial\mathbf{w} + \frac{1}{h}\langle \mathbf{F}^z \rangle \partial\bar{\mathbf{q}}_z \tag{B.11}$$

Substituting the expression of Eq. (B.11) into (B.10) it is possible to obtain:

$$\begin{aligned} \boldsymbol{\tau}_i^{\alpha}(\mathbf{x}, z) &= \bar{\mathbf{p}}^{(B)}(\mathbf{x}) \left(-1 - \frac{1}{h}(z + h/2) \right) - \frac{1}{h}(z + h/2)\bar{\mathbf{p}}^{(T)}(\mathbf{x}) + \hat{\mathbf{A}}^z(z)\partial\mathbf{e}(\mathbf{x}) + \hat{\mathbf{B}}^z(z)\partial\mathbf{k}(\mathbf{x}) + \hat{\mathbf{D}}^z(z)\partial\mathbf{k}^{\psi}(\mathbf{x}) + \hat{\mathbf{E}}^z(z)\partial\mathbf{w}(\mathbf{x}) + \hat{\mathbf{F}}^z(z)\partial\bar{\mathbf{q}}_z(\mathbf{x}) = \\ &= \mathbf{Z}_p(z)\bar{\mathbf{q}}_p(\mathbf{x}) + \mathbf{Z}_t(z)\mathbf{q}_t(\mathbf{x}) + \mathbf{Z}_{qz}(z)\partial\bar{\mathbf{q}}_z(\mathbf{x}) \end{aligned} \tag{B.12}$$

Where, the terms of (B.12) and (30) are defined as follows:

$$\begin{aligned}
\widehat{\mathbf{A}}^z(z) &= \mathbf{A}^z(z) - (z + h/2) \frac{1}{h} \langle \mathbf{A}^z \rangle \\
\widehat{\mathbf{B}}^z(z) &= \mathbf{B}^z(z) - (z + h/2) \frac{1}{h} \langle \mathbf{B}^z \rangle \\
\widehat{\mathbf{D}}^z(z) &= \mathbf{D}^z(z) - (z + h/2) \frac{1}{h} \langle \mathbf{D}^z \rangle \\
\widehat{\mathbf{E}}^z(z) &= \mathbf{E}^z(z) - (z + h/2) \frac{1}{h} \langle \mathbf{E}^z \rangle \\
\widehat{\mathbf{F}}^z(z) &= \mathbf{F}^z(z) - (z + h/2) \frac{1}{h} \langle \mathbf{F}^z \rangle \\
\mathbf{Z}_p(z) &= \left[\left(-1 - \frac{1}{h}(z + h/2) \right) \quad -\frac{1}{h}(z + h/2) \right] \\
\mathbf{Z}_t(z) &= [\widehat{\mathbf{A}}^z(z) \quad \widehat{\mathbf{B}}^z(z) \quad \widehat{\mathbf{D}}^z(z) \quad \widehat{\mathbf{E}}^z(z)] \\
\mathbf{Z}_{qz}(z) &= \widehat{\mathbf{F}}^z(z) \\
\bar{\mathbf{q}}_p(\mathbf{x})^T &= [\bar{\mathbf{p}}^{(B)} \quad \bar{\mathbf{p}}^{(T)}] = [p_{1(B)} \quad p_{2(B)} \quad p_{1(T)} \quad p_{2(T)}] \\
\mathbf{q}_t(\mathbf{x})^T &= [\partial \mathbf{e}^T \quad \partial \mathbf{k}^T \quad \partial \mathbf{k}^{wT} \quad \partial \mathbf{w}^T]
\end{aligned} \tag{B.13}$$

Appendix C

Full expression of the equilibrium equation and boundary condition terms

In this appendix are reported the full expressions of the terms appeared in the en-RZT_{3,2}^(m) equilibrium equations, i.e. Eqs. (41)–(57):

$$\begin{aligned}
\widehat{Q}^{w0} &= -\left(\widehat{D}_{11}^w w_{,11}^{(0)} + \widehat{D}_{12}^w w_{,11}^{(1)} + \widehat{D}_{13}^w w_{,11}^{(2)} + \widehat{D}_{14}^w w_{,12}^{(0)} + \widehat{D}_{15}^w w_{,12}^{(1)} + \widehat{D}_{16}^w w_{,12}^{(2)} + \widehat{D}_{11}^\theta \theta_{1,1} + \widehat{D}_{12}^\theta \theta_{2,1} + \widehat{D}_{11}^\psi \psi_{1,1} + \widehat{D}_{12}^\psi \psi_{2,1} \right) + \\
&\quad -\left(\widehat{D}_{41}^w w_{,12}^{(0)} + \widehat{D}_{42}^w w_{,12}^{(1)} + \widehat{D}_{43}^w w_{,12}^{(2)} + \widehat{D}_{44}^w w_{,22}^{(0)} + \widehat{D}_{45}^w w_{,22}^{(1)} + \widehat{D}_{46}^w w_{,22}^{(2)} + \widehat{D}_{41}^\theta \theta_{1,2} + \widehat{D}_{42}^\theta \theta_{2,2} + \widehat{D}_{41}^\psi \psi_{1,2} + \widehat{D}_{42}^\psi \psi_{2,2} \right) + \\
&\quad + \widehat{A}_{11}^{kw} e_{11,11} + \widehat{A}_{21}^{kw} e_{22,11} + \widehat{A}_{31}^{kw} e_{12,11} + \widehat{A}_{41}^{kw} e_{11,12} + \widehat{A}_{51}^{kw} e_{22,12} + \widehat{A}_{61}^{kw} e_{12,12} + \\
&\quad + \widehat{B}_{11}^{kw} k_{11,11} + \widehat{B}_{21}^{kw} k_{22,11} + \widehat{B}_{31}^{kw} k_{12,11} + \widehat{B}_{41}^{kw} k_{11,12} + \widehat{B}_{51}^{kw} k_{22,12} + \widehat{B}_{61}^{kw} k_{12,12} + \widehat{C}_{11}^{kw} k_{11,11}^\psi + \widehat{C}_{21}^{kw} k_{22,11}^\psi + \widehat{C}_{31}^{kw} k_{12,11}^\psi + \widehat{C}_{41}^{kw} k_{21,11}^\psi + \\
&\quad + \widehat{C}_{51}^{kw} k_{11,12}^\psi + \widehat{C}_{61}^{kw} k_{22,12}^\psi + \widehat{C}_{71}^{kw} k_{12,12}^\psi + \widehat{C}_{81}^{kw} k_{21,12}^\psi + \widehat{D}_{11}^{kw} w_{,11}^{(0)} + \widehat{D}_{12}^{kw} w_{,11}^{(1)} + \widehat{D}_{13}^{kw} w_{,11}^{(2)} + \widehat{D}_{14}^{kw} w_{,12}^{(0)} + \widehat{D}_{15}^{kw} w_{,12}^{(1)} + \widehat{D}_{16}^{kw} w_{,12}^{(2)} + \\
&\quad + \widehat{A}_{14}^{kw} e_{11,12} + \widehat{A}_{24}^{kw} e_{22,12} + \widehat{A}_{34}^{kw} e_{12,12} + \widehat{A}_{44}^{kw} e_{11,22} + \widehat{A}_{54}^{kw} e_{22,22} + \widehat{A}_{64}^{kw} e_{12,22} + \\
&\quad + \widehat{B}_{14}^{kw} k_{11,12} + \widehat{B}_{24}^{kw} k_{22,12} + \widehat{B}_{34}^{kw} k_{12,12} + \widehat{B}_{44}^{kw} k_{11,22} + \widehat{B}_{54}^{kw} k_{22,22} + \widehat{B}_{64}^{kw} k_{12,22} + \widehat{C}_{14}^{kw} k_{11,12}^\psi + \widehat{C}_{24}^{kw} k_{22,12}^\psi + \widehat{C}_{34}^{kw} k_{12,12}^\psi + \widehat{C}_{44}^{kw} k_{21,12}^\psi + \\
&\quad + \widehat{C}_{54}^{kw} k_{11,22}^\psi + \widehat{C}_{64}^{kw} k_{22,22}^\psi + \widehat{C}_{74}^{kw} k_{12,22}^\psi + \widehat{C}_{84}^{kw} k_{21,22}^\psi + \widehat{D}_{41}^{kw} w_{,12}^{(0)} + \widehat{D}_{42}^{kw} w_{,12}^{(1)} + \widehat{D}_{43}^{kw} w_{,12}^{(2)} + \widehat{D}_{44}^{kw} w_{,22}^{(0)} + \widehat{D}_{45}^{kw} w_{,22}^{(1)} + \widehat{D}_{46}^{kw} w_{,22}^{(2)} +
\end{aligned} \tag{C.1}$$

$$\begin{aligned}
\widehat{Q}^{w1} &= -\left(\widehat{D}_{11}^w w_{,11}^{(0)} + \widehat{D}_{12}^w w_{,11}^{(1)} + \widehat{D}_{13}^w w_{,11}^{(2)} + \widehat{D}_{14}^w w_{,12}^{(0)} + \widehat{D}_{15}^w w_{,12}^{(1)} + \widehat{D}_{16}^w w_{,12}^{(2)} + \widehat{D}_{11}^\theta \theta_{1,1} + \widehat{D}_{12}^\theta \theta_{2,1} + \widehat{D}_{11}^\psi \psi_{1,1} + \widehat{D}_{12}^\psi \psi_{2,1} \right) + \\
&\quad -\left(\widehat{D}_{51}^w w_{,12}^{(0)} + \widehat{D}_{52}^w w_{,12}^{(1)} + \widehat{D}_{53}^w w_{,12}^{(2)} + \widehat{D}_{54}^w w_{,22}^{(0)} + \widehat{D}_{55}^w w_{,22}^{(1)} + \widehat{D}_{56}^w w_{,22}^{(2)} + \widehat{D}_{51}^\theta \theta_{1,2} + \widehat{D}_{52}^\theta \theta_{2,2} + \widehat{D}_{51}^\psi \psi_{1,2} + \widehat{D}_{52}^\psi \psi_{2,2} \right) + \\
&\quad + \widehat{A}_{12}^{kw} e_{11,11} + \widehat{A}_{22}^{kw} e_{22,11} + \widehat{A}_{32}^{kw} e_{12,11} + \widehat{A}_{42}^{kw} e_{11,12} + \widehat{A}_{52}^{kw} e_{22,12} + \widehat{A}_{62}^{kw} e_{12,12} + \\
&\quad + \widehat{B}_{12}^{kw} k_{11,11} + \widehat{B}_{22}^{kw} k_{22,11} + \widehat{B}_{32}^{kw} k_{12,11} + \widehat{B}_{42}^{kw} k_{11,12} + \widehat{B}_{52}^{kw} k_{22,12} + \widehat{B}_{62}^{kw} k_{12,12} + \\
&\quad + \widehat{C}_{12}^{kw} k_{11,11}^\psi + \widehat{C}_{22}^{kw} k_{22,11}^\psi + \widehat{C}_{32}^{kw} k_{12,11}^\psi + \widehat{C}_{41}^{kw} k_{22,11}^\psi + \widehat{C}_{52}^{kw} k_{11,12}^\psi + \widehat{C}_{62}^{kw} k_{22,12}^\psi + \widehat{C}_{72}^{kw} k_{12,12}^\psi + \widehat{C}_{82}^{kw} k_{21,12}^\psi + \\
&\quad + \widehat{D}_{21}^{kw} w_{,11}^{(0)} + \widehat{D}_{22}^{kw} w_{,11}^{(1)} + \widehat{D}_{23}^{kw} w_{,11}^{(2)} + \widehat{D}_{24}^{kw} w_{,12}^{(0)} + \widehat{D}_{25}^{kw} w_{,12}^{(1)} + \widehat{D}_{26}^{kw} w_{,12}^{(2)} + \\
&\quad + \widehat{A}_{15}^{kw} e_{11,12} + \widehat{A}_{25}^{kw} e_{22,12} + \widehat{A}_{35}^{kw} e_{12,12} + \widehat{A}_{45}^{kw} e_{11,22} + \widehat{A}_{55}^{kw} e_{22,22} + \widehat{A}_{65}^{kw} e_{12,22} + \\
&\quad + \widehat{B}_{15}^{kw} k_{11,12} + \widehat{B}_{25}^{kw} k_{22,12} + \widehat{B}_{35}^{kw} k_{12,12} + \widehat{B}_{45}^{kw} k_{11,22} + \widehat{B}_{55}^{kw} k_{22,22} + \widehat{B}_{65}^{kw} k_{12,22} + \\
&\quad + \widehat{C}_{15}^{kw} k_{11,12}^\psi + \widehat{C}_{25}^{kw} k_{22,12}^\psi + \widehat{C}_{35}^{kw} k_{12,12}^\psi + \widehat{C}_{45}^{kw} k_{21,12}^\psi + \widehat{C}_{55}^{kw} k_{11,22}^\psi + \widehat{C}_{65}^{kw} k_{22,22}^\psi + \widehat{C}_{75}^{kw} k_{12,22}^\psi + \widehat{C}_{85}^{kw} k_{21,22}^\psi + \\
&\quad + \widehat{D}_{51}^{kw} w_{,12}^{(0)} + \widehat{D}_{52}^{kw} w_{,12}^{(1)} + \widehat{D}_{53}^{kw} w_{,12}^{(2)} + \widehat{D}_{54}^{kw} w_{,22}^{(0)} + \widehat{D}_{55}^{kw} w_{,22}^{(1)} + \widehat{D}_{56}^{kw} w_{,22}^{(2)} +
\end{aligned} \tag{C.2}$$

$$\begin{aligned}
 K_{\psi 12}^{HR} = & \widehat{C}_{31}^w w_{,11}^{(0)} + \widehat{C}_{32}^w w_{,11}^{(1)} + \widehat{C}_{33}^w w_{,11}^{(2)} + \widehat{C}_{34}^w w_{,12}^{(0)} + \widehat{C}_{35}^w w_{,12}^{(1)} + \widehat{C}_{36}^w w_{,12}^{(2)} + \widehat{C}_{31}^\theta \theta_{1,1} + \widehat{C}_{32}^\theta \theta_{2,1} + \widehat{C}_{31}^\psi \psi_{1,1} + \widehat{C}_{32}^\psi \psi_{2,1} + \\
 & + \widehat{C}_{71}^w w_{,12}^{(0)} + \widehat{C}_{72}^w w_{,12}^{(1)} + \widehat{C}_{73}^w w_{,12}^{(2)} + \widehat{C}_{74}^w w_{,22}^{(0)} + \widehat{C}_{75}^w w_{,22}^{(1)} + \widehat{C}_{76}^w w_{,22}^{(2)} + \widehat{C}_{71}^\theta \theta_{1,2} + \widehat{C}_{72}^\theta \theta_{2,2} + \widehat{C}_{71}^\psi \psi_{1,2} + \widehat{C}_{72}^\psi \psi_{2,2} + \\
 & \left(\widehat{C}_{31}^p \bar{p}_{1(B),1} + \widehat{C}_{32}^p \bar{p}_{2(B),1} + \widehat{C}_{33}^p \bar{p}_{1(T),1} + \widehat{C}_{34}^p \bar{p}_{2(T),1} + \widehat{A}_{13}^{kw} e_{11,11} + \widehat{A}_{23}^{kw} e_{22,11} + \widehat{A}_{33}^{kw} e_{12,11} + \widehat{A}_{43}^{kw} e_{11,12} + \widehat{A}_{53}^{kw} e_{22,12} + \widehat{A}_{63}^{kw} e_{12,12} + \right. \\
 & + \widehat{B}_{13}^{kw} k_{11,11} + \widehat{B}_{23}^{kw} k_{22,11} + \widehat{B}_{33}^{kw} k_{12,11} + \widehat{B}_{43}^{kw} k_{11,12} + \widehat{B}_{53}^{kw} k_{22,12} + \widehat{B}_{63}^{kw} k_{12,12} + \\
 & + \widehat{C}_{31}^{kw} k_{11,11}^{(0)} + \widehat{C}_{32}^{kw} k_{11,11}^{(1)} + \widehat{C}_{33}^{kw} k_{11,11}^{(2)} + \widehat{C}_{34}^{kw} k_{12,11}^{(0)} + \widehat{C}_{35}^{kw} k_{12,11}^{(1)} + \widehat{C}_{36}^{kw} k_{12,11}^{(2)} + \widehat{C}_{37}^{kw} k_{12,12}^{(0)} + \widehat{C}_{38}^{kw} k_{12,12}^{(1)} + \\
 & + \widehat{C}_{31}^{kw} w_{,11}^{(0)} + \widehat{C}_{32}^{kw} w_{,11}^{(1)} + \widehat{C}_{33}^{kw} w_{,11}^{(2)} + \widehat{C}_{34}^{kw} w_{,12}^{(0)} + \widehat{C}_{35}^{kw} w_{,12}^{(1)} + \widehat{C}_{36}^{kw} w_{,12}^{(2)} + \\
 & + \widehat{C}_{71}^p \bar{p}_{1(B),2} + \widehat{C}_{72}^p \bar{p}_{2(B),2} + \widehat{C}_{73}^p \bar{p}_{1(T),2} + \widehat{C}_{74}^p \bar{p}_{2(T),2} + \widehat{A}_{17}^{kw} e_{11,12} + \widehat{A}_{27}^{kw} e_{22,12} + \widehat{A}_{37}^{kw} e_{12,12} + \widehat{A}_{47}^{kw} e_{11,22} + \widehat{A}_{57}^{kw} e_{22,22} + \widehat{A}_{67}^{kw} e_{12,22} + \\
 & + \widehat{B}_{17}^{kw} k_{11,12} + \widehat{B}_{27}^{kw} k_{22,12} + \widehat{B}_{37}^{kw} k_{12,12} + \widehat{B}_{47}^{kw} k_{11,22} + \widehat{B}_{57}^{kw} k_{22,22} + \widehat{B}_{67}^{kw} k_{12,22} + \\
 & + \widehat{C}_{71}^{kw} k_{11,12}^{(0)} + \widehat{C}_{72}^{kw} k_{11,12}^{(1)} + \widehat{C}_{73}^{kw} k_{11,12}^{(2)} + \widehat{C}_{74}^{kw} k_{12,12}^{(0)} + \widehat{C}_{75}^{kw} k_{12,12}^{(1)} + \widehat{C}_{76}^{kw} k_{12,12}^{(2)} + \widehat{C}_{77}^{kw} k_{12,22}^{(0)} + \widehat{C}_{78}^{kw} k_{12,22}^{(1)} + \\
 & + \widehat{C}_{71}^{kw} w_{,12}^{(0)} + \widehat{C}_{72}^{kw} w_{,12}^{(1)} + \widehat{C}_{73}^{kw} w_{,12}^{(2)} + \widehat{C}_{74}^{kw} w_{,22}^{(0)} + \widehat{C}_{75}^{kw} w_{,22}^{(1)} + \widehat{C}_{76}^{kw} w_{,22}^{(2)} + \\
 & \left. \widehat{C}_{31}^q \bar{p}_{3(B),11} + \widehat{C}_{32}^q \bar{p}_{3(T),11} + \widehat{C}_{33}^q \bar{p}_{3(B),12} + \widehat{C}_{34}^q \bar{p}_{3(T),12} + \widehat{C}_{71}^q \bar{p}_{3(B),12} + \widehat{C}_{72}^q \bar{p}_{3(T),12} + \widehat{C}_{73}^q \bar{p}_{3(B),22} + \widehat{C}_{74}^q \bar{p}_{3(T),22} \right)
 \end{aligned} \tag{C.12}$$

$$\begin{aligned}
 K_{\psi 21}^{HR} = & \widehat{C}_{41}^w w_{,11}^{(0)} + \widehat{C}_{42}^w w_{,11}^{(1)} + \widehat{C}_{43}^w w_{,11}^{(2)} + \widehat{C}_{44}^w w_{,12}^{(0)} + \widehat{C}_{45}^w w_{,12}^{(1)} + \widehat{C}_{46}^w w_{,12}^{(2)} + \widehat{C}_{41}^\theta \theta_{1,1} + \widehat{C}_{42}^\theta \theta_{2,1} + \widehat{C}_{41}^\psi \psi_{1,1} + \widehat{C}_{42}^\psi \psi_{2,1} + \\
 & + \widehat{C}_{81}^w w_{,12}^{(0)} + \widehat{C}_{82}^w w_{,12}^{(1)} + \widehat{C}_{83}^w w_{,12}^{(2)} + \widehat{C}_{84}^w w_{,22}^{(0)} + \widehat{C}_{85}^w w_{,22}^{(1)} + \widehat{C}_{86}^w w_{,22}^{(2)} + \widehat{C}_{81}^\theta \theta_{1,2} + \widehat{C}_{82}^\theta \theta_{2,2} + \widehat{C}_{81}^\psi \psi_{1,2} + \widehat{C}_{82}^\psi \psi_{2,2} + \\
 & \left(\widehat{C}_{41}^p \bar{p}_{1(B),1} + \widehat{C}_{42}^p \bar{p}_{2(B),1} + \widehat{C}_{43}^p \bar{p}_{1(T),1} + \widehat{C}_{44}^p \bar{p}_{2(T),1} + \widehat{A}_{14}^{kw} e_{11,11} + \widehat{A}_{24}^{kw} e_{22,11} + \widehat{A}_{34}^{kw} e_{12,11} + \widehat{A}_{44}^{kw} e_{11,12} + \widehat{A}_{54}^{kw} e_{22,12} + \widehat{A}_{64}^{kw} e_{12,12} + \right. \\
 & + \widehat{B}_{14}^{kw} k_{11,11} + \widehat{B}_{24}^{kw} k_{22,11} + \widehat{B}_{34}^{kw} k_{12,11} + \widehat{B}_{44}^{kw} k_{11,12} + \widehat{B}_{54}^{kw} k_{22,12} + \widehat{B}_{64}^{kw} k_{12,12} + \\
 & + \widehat{C}_{41}^{kw} k_{11,11}^{(0)} + \widehat{C}_{42}^{kw} k_{11,11}^{(1)} + \widehat{C}_{43}^{kw} k_{11,11}^{(2)} + \widehat{C}_{44}^{kw} k_{12,11}^{(0)} + \widehat{C}_{45}^{kw} k_{12,11}^{(1)} + \widehat{C}_{46}^{kw} k_{12,11}^{(2)} + \widehat{C}_{47}^{kw} k_{12,12}^{(0)} + \widehat{C}_{48}^{kw} k_{12,12}^{(1)} + \\
 & + \widehat{C}_{41}^{kw} w_{,11}^{(0)} + \widehat{C}_{42}^{kw} w_{,11}^{(1)} + \widehat{C}_{43}^{kw} w_{,11}^{(2)} + \widehat{C}_{44}^{kw} w_{,12}^{(0)} + \widehat{C}_{45}^{kw} w_{,12}^{(1)} + \widehat{C}_{46}^{kw} w_{,12}^{(2)} + \\
 & + \widehat{C}_{81}^p \bar{p}_{1(B),2} + \widehat{C}_{82}^p \bar{p}_{2(B),2} + \widehat{C}_{83}^p \bar{p}_{1(T),2} + \widehat{C}_{84}^p \bar{p}_{2(T),2} + \widehat{A}_{18}^{kw} e_{11,12} + \widehat{A}_{28}^{kw} e_{22,12} + \widehat{A}_{38}^{kw} e_{12,12} + \widehat{A}_{48}^{kw} e_{11,22} + \widehat{A}_{58}^{kw} e_{22,22} + \widehat{A}_{68}^{kw} e_{12,22} + \\
 & + \widehat{B}_{18}^{kw} k_{11,12} + \widehat{B}_{28}^{kw} k_{22,12} + \widehat{B}_{38}^{kw} k_{12,12} + \widehat{B}_{48}^{kw} k_{11,22} + \widehat{B}_{58}^{kw} k_{22,22} + \widehat{B}_{68}^{kw} k_{12,22} + \\
 & + \widehat{C}_{81}^{kw} k_{11,12}^{(0)} + \widehat{C}_{82}^{kw} k_{11,12}^{(1)} + \widehat{C}_{83}^{kw} k_{11,12}^{(2)} + \widehat{C}_{84}^{kw} k_{12,12}^{(0)} + \widehat{C}_{85}^{kw} k_{12,12}^{(1)} + \widehat{C}_{86}^{kw} k_{12,12}^{(2)} + \widehat{C}_{87}^{kw} k_{12,22}^{(0)} + \widehat{C}_{88}^{kw} k_{12,22}^{(1)} + \\
 & + \widehat{C}_{81}^{kw} w_{,12}^{(0)} + \widehat{C}_{82}^{kw} w_{,12}^{(1)} + \widehat{C}_{83}^{kw} w_{,12}^{(2)} + \widehat{C}_{84}^{kw} w_{,22}^{(0)} + \widehat{C}_{85}^{kw} w_{,22}^{(1)} + \widehat{C}_{86}^{kw} w_{,22}^{(2)} + \\
 & \left. + \widehat{C}_{41}^q \bar{p}_{3(B),11} + \widehat{C}_{42}^q \bar{p}_{3(T),11} + \widehat{C}_{43}^q \bar{p}_{3(B),12} + \widehat{C}_{44}^q \bar{p}_{3(T),12} + \widehat{C}_{81}^q \bar{p}_{3(B),12} + \widehat{C}_{82}^q \bar{p}_{3(T),12} + \widehat{C}_{83}^q \bar{p}_{3(B),22} + \widehat{C}_{84}^q \bar{p}_{3(T),22} \right)
 \end{aligned} \tag{C.13}$$

Furthermore, the terms shown in the boundary condition expression, i.e. Eq. (58), can read:

$$\begin{aligned}
 {}^{HR} \bar{\mathbf{E}} = & \widehat{\mathbf{A}}^w \partial \mathbf{w} + \widehat{\mathbf{A}}^\theta \boldsymbol{\theta} + \widehat{\mathbf{A}}^\psi \boldsymbol{\psi} - (\widehat{\mathbf{A}}^p \bar{\mathbf{p}} + \widehat{\mathbf{A}}^e \partial \mathbf{e} + \widehat{\mathbf{A}}^k \partial \mathbf{k} + \widehat{\mathbf{A}}^{kw} \partial \mathbf{k}^\psi + \widehat{\mathbf{A}}^{kw} \partial \mathbf{w} + \widehat{\mathbf{A}}^q \partial \bar{\mathbf{q}}_z) {}^{HR} \bar{\mathbf{K}} \\
 = & \widehat{\mathbf{B}}^w \partial \mathbf{w} + \widehat{\mathbf{B}}^\theta \boldsymbol{\theta} + \widehat{\mathbf{B}}^\psi \boldsymbol{\psi} - (\widehat{\mathbf{B}}^p \bar{\mathbf{p}} + \widehat{\mathbf{A}}^{kT} \partial \mathbf{e} + \widehat{\mathbf{B}}^k \partial \mathbf{k} + \widehat{\mathbf{B}}^{kw} \partial \mathbf{k}^\psi + \widehat{\mathbf{B}}^{kw} \partial \mathbf{w} + \widehat{\mathbf{B}}^q \partial \bar{\mathbf{q}}_z) {}^{HR} \bar{\mathbf{K}} \\
 = & \widehat{\mathbf{C}}^w \partial \mathbf{w} + \widehat{\mathbf{C}}^\theta \boldsymbol{\theta} + \widehat{\mathbf{C}}^\psi \boldsymbol{\psi} - (\widehat{\mathbf{C}}^p \bar{\mathbf{p}} + \widehat{\mathbf{A}}^{kwT} \partial \mathbf{e} + \widehat{\mathbf{B}}^{kwT} \partial \mathbf{k} + \widehat{\mathbf{C}}^{kw} \partial \mathbf{k}^\psi + \widehat{\mathbf{C}}^{kw} \partial \mathbf{w} + \widehat{\mathbf{C}}^q \partial \bar{\mathbf{q}}_z) {}^{HR} \bar{\mathbf{Q}} \\
 = & \widehat{\mathbf{D}}^w \partial \mathbf{w} + \widehat{\mathbf{D}}^\theta \boldsymbol{\theta} + \widehat{\mathbf{D}}^\psi \boldsymbol{\psi} - (\widehat{\mathbf{D}}^p \bar{\mathbf{p}} + \widehat{\mathbf{A}}^{kwT} \partial \mathbf{e} + \widehat{\mathbf{B}}^{kwT} \partial \mathbf{k} + \widehat{\mathbf{C}}^{kwT} \partial \mathbf{k}^\psi + \widehat{\mathbf{D}}^{kw} \partial \mathbf{w} + \widehat{\mathbf{D}}^q \partial \bar{\mathbf{q}}_z)
 \end{aligned} \tag{C.14}$$

where

$$\begin{aligned}
 {}^{HR} \bar{\mathbf{E}}^T = & \left[{}^{HR} \bar{E}_1^{e11} \quad {}^{HR} \bar{E}_1^{e22} \quad {}^{HR} \bar{E}_1^{e12} \quad {}^{HR} \bar{E}_2^{e11} \quad {}^{HR} \bar{E}_2^{e22} \quad {}^{HR} \bar{E}_2^{e12} \right]; \quad {}^{HR} \bar{\mathbf{K}}^T = \left[{}^{HR} \bar{K}_1^{k11} \quad {}^{HR} \bar{K}_1^{k22} \quad {}^{HR} \bar{K}_1^{k12} \quad {}^{HR} \bar{K}_2^{k11} \quad {}^{HR} \bar{K}_2^{k22} \quad {}^{HR} \bar{K}_2^{k12} \right]; \quad {}^{HR} \bar{\mathbf{K}}^{\psi T} \\
 = & \left[{}^{HR} \bar{K}_1^{k1\psi} \quad {}^{HR} \bar{K}_1^{k2\psi} \quad {}^{HR} \bar{K}_1^{k1\psi} \quad {}^{HR} \bar{K}_2^{k2\psi} \quad {}^{HR} \bar{K}_2^{k1\psi} \quad {}^{HR} \bar{K}_2^{k2\psi} \quad {}^{HR} \bar{K}_2^{k1\psi} \quad {}^{HR} \bar{K}_2^{k2\psi} \right]; \quad {}^{HR} \bar{\mathbf{Q}}^T \\
 = & \left[{}^{HR} \bar{Q}_1^{w0} \quad {}^{HR} \bar{Q}_1^{w1} \quad {}^{HR} \bar{Q}_1^{w2} \quad {}^{HR} \bar{Q}_2^{w0} \quad {}^{HR} \bar{Q}_2^{w1} \quad {}^{HR} \bar{Q}_2^{w2} \right]
 \end{aligned} \tag{C.15}$$

Appendix D

Matrices definition of the en-RZT^(m)_{3,2} constitutive relations

In this appendix are resumed the matrices definitions of the constitutive relations for resultants of forces and moments:

$$\begin{aligned}
 \tilde{\mathbf{A}} &= \langle \mathbf{Q}_p^{(k)} + \mathbf{R}^{(k)T} \mathbf{A}_\sigma^u \rangle; \quad \tilde{\mathbf{B}} = \langle z \mathbf{Q}_p^{(k)} + \mathbf{R}^{(k)T} \mathbf{A}_\sigma^\theta \rangle; \quad \tilde{\mathbf{A}}^\phi = \langle \mathbf{Q}_p^{(k)} \mathbf{M}^{(k)} + \mathbf{R}^{(k)T} \mathbf{A}_\sigma^\psi \rangle; \\
 \tilde{\mathbf{A}}^w &= \langle \mathbf{R}^{(k)T} \mathbf{A}_\sigma^w \rangle; \quad \tilde{\mathbf{A}}^{qz} = \langle \mathbf{R}^{(k)T} \mathbf{A}_\sigma^{qz} \rangle; \\
 \tilde{\mathbf{C}} &= \langle z \mathbf{Q}_p^{(k)} + z \mathbf{R}^{(k)T} \mathbf{A}_\sigma^u \rangle; \quad \tilde{\mathbf{D}} = \langle z^2 \mathbf{Q}_p^{(k)} + z \mathbf{R}^{(k)T} \mathbf{A}_\sigma^\theta \rangle; \quad \tilde{\mathbf{B}}^\phi = \langle z \mathbf{Q}_p^{(k)} \mathbf{M}^{(k)} + z \mathbf{R}^{(k)T} \mathbf{A}_\sigma^\psi \rangle; \\
 \tilde{\mathbf{B}}^w &= \langle z \mathbf{R}^{(k)T} \mathbf{A}_\sigma^w \rangle; \quad \tilde{\mathbf{B}}^{qz} = \langle z \mathbf{R}^{(k)T} \mathbf{A}_\sigma^{qz} \rangle; \\
 \tilde{\mathbf{E}}^\phi &= \langle \mathbf{M}^{(k)T} \mathbf{Q}_p^{(k)} + \mathbf{M}^{(k)T} \mathbf{R}^{(k)T} \mathbf{A}_\sigma^u \rangle; \quad \tilde{\mathbf{F}}^\phi = \langle z \mathbf{M}^{(k)T} \mathbf{Q}_p^{(k)} + \mathbf{M}^{(k)T} \mathbf{R}^{(k)T} \mathbf{A}_\sigma^\theta \rangle; \quad \tilde{\mathbf{G}}^\phi = \langle \mathbf{M}^{(k)T} \mathbf{Q}_p^{(k)} \mathbf{M}^{(k)} + \mathbf{M}^{(k)T} \mathbf{R}^{(k)T} \mathbf{A}_\sigma^\psi \rangle; \\
 \tilde{\mathbf{C}}^w &= \langle \mathbf{M}^{(k)T} \mathbf{R}^{(k)T} \mathbf{A}_\sigma^w \rangle; \quad \tilde{\mathbf{C}}^{qz} = \langle \mathbf{M}^{(k)T} \mathbf{R}^{(k)T} \mathbf{A}_\sigma^{qz} \rangle \\
 \mathbf{A}^{Nz} &= \langle \mathbf{H}_z^T \mathbf{A}_\sigma^u \rangle; \quad \mathbf{B}^{Nz} = \langle \mathbf{H}_z^T \mathbf{A}_\sigma^\theta \rangle; \quad \mathbf{C}^{Nz} = \langle \mathbf{H}_z^T \mathbf{A}_\sigma^\psi \rangle; \quad \mathbf{D}^{Nz} = \langle \mathbf{H}_z^T \mathbf{A}_\sigma^w \rangle; \quad \mathbf{E}^{Nz} = \langle \mathbf{H}_z^T \mathbf{A}_\sigma^{qz} \rangle
 \end{aligned}
 \tag{D.1}$$

From the HR statement linked to the transverse shear strain compatibility, it appears the following constitutive matrices:

$$\begin{aligned}
 \hat{\mathbf{A}}^w &= \langle \hat{\mathbf{A}}^z \mathbf{H}^z \rangle; \quad \hat{\mathbf{A}}^\theta = \langle \hat{\mathbf{A}}^z \rangle; \quad \hat{\mathbf{A}}^\psi = \langle \hat{\mathbf{A}}^z \partial_z \boldsymbol{\mu}^{(k)} \rangle; \quad \hat{\mathbf{A}}^p = \langle \hat{\mathbf{A}}^z \mathbf{S}_t^{(k)} \mathbf{Z}_p \rangle; \quad \hat{\mathbf{A}}^e = \langle \hat{\mathbf{A}}^z \mathbf{S}_t^{(k)} \hat{\mathbf{A}}^z \rangle; \\
 \hat{\mathbf{A}}^k &= \langle \hat{\mathbf{A}}^z \mathbf{S}_t^{(k)} \hat{\mathbf{B}}^z \rangle; \quad \hat{\mathbf{A}}^{kw} = \langle \hat{\mathbf{A}}^z \mathbf{S}_t^{(k)} \hat{\mathbf{D}}^z \rangle; \quad \hat{\mathbf{A}}^{kw} = \langle \hat{\mathbf{A}}^z \mathbf{S}_t^{(k)} \hat{\mathbf{E}}^z \rangle; \quad \hat{\mathbf{A}}^q = \langle \hat{\mathbf{A}}^z \mathbf{S}_t^{(k)} \hat{\mathbf{F}}^z \rangle; \\
 \hat{\mathbf{B}}^w &= \langle \hat{\mathbf{B}}^z \mathbf{H}^z \rangle; \quad \hat{\mathbf{B}}^\theta = \langle \hat{\mathbf{B}}^z \rangle; \quad \hat{\mathbf{B}}^\psi = \langle \hat{\mathbf{B}}^z \partial_z \boldsymbol{\mu}^{(k)} \rangle; \quad \hat{\mathbf{B}}^p = \langle \hat{\mathbf{B}}^z \mathbf{S}_t^{(k)} \mathbf{Z}_p \rangle; \quad \hat{\mathbf{B}}^e = \hat{\mathbf{A}}^{kT} = \langle \hat{\mathbf{B}}^z \mathbf{S}_t^{(k)} \hat{\mathbf{A}}^z \rangle; \\
 \hat{\mathbf{B}}^k &= \langle \hat{\mathbf{B}}^z \mathbf{S}_t^{(k)} \hat{\mathbf{B}}^z \rangle; \quad \hat{\mathbf{B}}^{kw} = \langle \hat{\mathbf{B}}^z \mathbf{S}_t^{(k)} \hat{\mathbf{D}}^z \rangle; \quad \hat{\mathbf{B}}^{kw} = \langle \hat{\mathbf{B}}^z \mathbf{S}_t^{(k)} \hat{\mathbf{E}}^z \rangle; \quad \hat{\mathbf{B}}^q = \langle \hat{\mathbf{B}}^z \mathbf{S}_t^{(k)} \hat{\mathbf{F}}^z \rangle; \\
 \hat{\mathbf{C}}^w &= \langle \hat{\mathbf{D}}^z \mathbf{H}^z \rangle; \quad \hat{\mathbf{C}}^\theta = \langle \hat{\mathbf{D}}^z \rangle; \quad \hat{\mathbf{C}}^\psi = \langle \hat{\mathbf{D}}^z \partial_z \boldsymbol{\mu}^{(k)} \rangle; \quad \hat{\mathbf{C}}^p = \langle \hat{\mathbf{D}}^z \mathbf{S}_t^{(k)} \mathbf{Z}_p \rangle; \quad \hat{\mathbf{C}}^e = \hat{\mathbf{A}}^{kwT} = \langle \hat{\mathbf{D}}^z \mathbf{S}_t^{(k)} \hat{\mathbf{A}}^z \rangle; \\
 \hat{\mathbf{C}}^k &= \hat{\mathbf{B}}^{kwT} = \langle \hat{\mathbf{D}}^z \mathbf{S}_t^{(k)} \hat{\mathbf{B}}^z \rangle; \quad \hat{\mathbf{C}}^{kw} = \langle \hat{\mathbf{D}}^z \mathbf{S}_t^{(k)} \hat{\mathbf{D}}^z \rangle; \quad \hat{\mathbf{C}}^{kw} = \langle \hat{\mathbf{D}}^z \mathbf{S}_t^{(k)} \hat{\mathbf{E}}^z \rangle; \quad \hat{\mathbf{C}}^q = \langle \hat{\mathbf{D}}^z \mathbf{S}_t^{(k)} \hat{\mathbf{F}}^z \rangle; \\
 \hat{\mathbf{D}}^w &= \langle \hat{\mathbf{E}}^z \mathbf{H}^z \rangle; \quad \hat{\mathbf{D}}^\theta = \langle \hat{\mathbf{E}}^z \rangle; \quad \hat{\mathbf{D}}^\psi = \langle \hat{\mathbf{E}}^z \partial_z \boldsymbol{\mu}^{(k)} \rangle; \quad \hat{\mathbf{D}}^p = \langle \hat{\mathbf{E}}^z \mathbf{S}_t^{(k)} \mathbf{Z}_p \rangle; \quad \hat{\mathbf{D}}^e = \hat{\mathbf{A}}^{kwT} = \langle \hat{\mathbf{E}}^z \mathbf{S}_t^{(k)} \hat{\mathbf{A}}^z \rangle; \\
 \hat{\mathbf{D}}^k &= \hat{\mathbf{B}}^{kwT} = \langle \hat{\mathbf{E}}^z \mathbf{S}_t^{(k)} \hat{\mathbf{B}}^z \rangle; \quad \hat{\mathbf{D}}^{kw} = \hat{\mathbf{C}}^{kwT} = \langle \hat{\mathbf{E}}^z \mathbf{S}_t^{(k)} \hat{\mathbf{D}}^z \rangle; \quad \hat{\mathbf{D}}^{kw} = \langle \hat{\mathbf{E}}^z \mathbf{S}_t^{(k)} \hat{\mathbf{E}}^z \rangle; \quad \hat{\mathbf{D}}^q = \langle \hat{\mathbf{E}}^z \mathbf{S}_t^{(k)} \hat{\mathbf{F}}^z \rangle; \\
 \hat{\mathbf{E}}^w &= \langle \hat{\mathbf{H}}^z \mathbf{F}^z \rangle; \quad \hat{\mathbf{E}}^\theta = \langle \hat{\mathbf{F}}^z \rangle; \quad \hat{\mathbf{E}}^\psi = \langle \partial_z \boldsymbol{\mu}^{(k)T} \hat{\mathbf{F}}^z \rangle;
 \end{aligned}
 \tag{D.2}$$

References

[1] Pagano NJ. Exact solutions for composite laminates in cylindrical bending. *J Thermoplast Compos Mater* 1969;3(3):398–411.

[2] Pagano NJ. Exact solutions for rectangular bidirectional composites and sandwich plates. *J Thermoplast Compos Mater* 1970;4(1):20–34.

[3] Pagano NJ. Influence of shear coupling in cylindrical bending of anisotropic laminates. *J Thermoplast Compos Mater* 1970;4(3):330–43.

[4] Noor AK, Burton WS. Three-dimensional solutions for antisymmetrically laminated anisotropic plates. *J Appl Mech* 1990;57(1):182–8.

[5] Savoia M, Reddy JN. A variational approach to three-dimensional elasticity solutions of laminated composite plates. *J Appl Mech* 1992;59(2S):S166–75.

[6] Reddy JN. *Mechanics of laminated composite plates and shells: Theory and analysis*. CRC Press; 2003.

[7] Abrate S, Di Sciuva M. Multilayer models for composite and sandwich structures. In: Beaumont PWR, Zweben CH, editors. *Comprehensive composite materials II*. Elsevier; 2018. p. 399–425.

[8] Abrate S, Di Sciuva M. Equivalent single layer theories for composite and sandwich structures: a review. *Compos Struct* 2017;179:482–94.

[9] Li D. Layerwise theories of laminated composite structures and their applications: a review. *Arch Comput Methods Eng* 2021;28(2):577–600.

[10] Di Sciuva M. Bending, vibration and buckling of simply supported thick multilayered orthotropic plates: an evaluation of a new displacement model. *J Sound Vib* 1986;105(3):425–42.

[11] Di Sciuva M. An improved shear-deformation theory for moderately thick multilayered anisotropic shells and plates. *J Appl Mech* 1987;54(3):589–96.

[12] Cho M, Parmerter R. Efficient higher order composite plate theory for general lamination configurations. *AIAA J* 1993;31(7):1299–306.

[13] Murakami H. Laminated composite plate theory with improved in-plane responses. *J Appl Mech* 1986;53(3):661–6.

[14] Icardi U. A three-dimensional Zig-Zag Theory for analysis of thick laminated beams. *Compos Struct* 2001;52(1):123–35.

[15] Tessler A, Di Sciuva M, Gherlone M. Refined Zigzag Theory for Laminated Composite and Sandwich Plates. *NASATP-2009-215561*. 2009. p. 1–53.

[16] Tessler A, Di Sciuva M, Gherlone M. Refinement of Timoshenko Beam Theory for Composite and Sandwich Beams Using Zigzag Kinematics. *NASATP-2007-215086*. 2007. p. 1–45.

[17] Eijo A, Onate E, Oller S. A numerical model of delamination in composite laminated beams using the LRZ beam element based on the refined Zigzag Theory. *Compos Struct* 2013;104:270–80.

[18] Di Sciuva M, Gherlone M, Iurlaro L, Tessler A. A class of higher-order C^0 composite and sandwich beam elements based on the refined Zigzag Theory. *Compos Struct* 2015;132:784–803.

[19] Dorduncu M. Stress analysis of laminated composite beams using refined Zigzag Theory and peridynamic differential operator. *Compos Struct* 2019;218:193–203.

[20] Wimmer H, Nachbagger K. Exact transfer- and stiffness matrix for the composite beam-column with refined zigzag kinematics. *Compos Struct* 2018;189:700–6.

[21] Iurlaro L, Gherlone M, Di Sciuva M, Tessler A. Assessment of the refined Zigzag Theory for bending, vibration, and buckling of sandwich plates: a comparative study of different theories. *Compos Struct* 2013;106:777–92.

[22] Eijo A, Onate E, Oller S. A four-noded quadrilateral element for composite laminated plates/shells using the refined Zigzag Theory. *Int J Numer Methods Eng* 2013;95(8):631–60.

[23] Iurlaro L, Gherlone M, Di Sciuva M. Bending and free vibration analysis of functionally graded sandwich plates using the refined Zigzag Theory. *J Sandw Struct Mater* 2014;16(6):669–99.

[24] Di Sciuva M, Sorrenti M. Bending, free vibration and buckling of functionally graded carbon nanotube-reinforced sandwich plates, using the extended refined Zigzag Theory. *Compos Struct* 2019;227:1–20.

[25] Versino D, Gherlone M, Mattone MC, Di Sciuva M, Tessler A. C^0 triangular elements based on the refined Zigzag Theory for multilayered composite and sandwich plates. *Compos Part B Eng* 2013;44(1):218–30.

[26] Versino D, Gherlone M, Di Sciuva M. Four-node shell element for doubly curved multilayered composites based on the refined Zigzag Theory. *Compos Struct* 2014;118:392–402.

[27] Gherlone M, Versino D, Zarra V. Multilayered triangular and quadrilateral flat shell elements based on the refined Zigzag Theory. *Compos Struct* 2019;233:1–16.

[28] Whitney JM. Bending-extensional coupling in laminated plates under transverse loading. *J Thermoplast Compos Mater* 1969;3(1):20–8.

[29] Di Sciuva M. A refined transverse shear deformation theory for multilayered anisotropic plates. *Atti Accad Delle Sci Torino* 1984;118:279–95.

[30] Loredo A, Castel A. A multilayer anisotropic plate model with warping functions for the study of vibrations reformulated from Woodcock’s work. *J Sound Vib* 2013;332(1):102–25.

[31] Loredo A, Castel A. Two multilayered plate models with transverse shear warping functions issued from three dimensional elasticity equations. *Compos Struct* 2014;117:382–95.

[32] Loredo A. A multilayered plate theory with transverse shear and normal warping functions. *Compos Struct* 2016;156:361–74.

[33] Loredo A, D’Ottavio M, Vidal P, Polit O. A family of higher-order single layer plate models meeting C_2^0 -requirements for arbitrary laminates. *Compos Struct* 2019;225:14.

[34] Sorrenti M, Di Sciuva M. An enhancement of the warping shear functions of refined Zigzag Theory. *J Appl Mech* 2021;88(8):7.

[35] Sorrenti M, Gherlone M, Di Sciuva M. Free vibration analysis of angle-ply laminated and sandwich plates using enhanced refined Zigzag Theory. In: *19th International Conference of Numerical Analysis and Applied Mechanics*, Rhodes, Greece; 2021.

- [36] Noor AK, Burton WS, Bert CW. Computational models for sandwich panels and shells. *Appl Mech Rev* 1996;49(3):155–99.
- [37] Barut A, Madenci E, Tessler A. A refined Zigzag Theory for laminated composite and sandwich plates incorporating thickness stretch deformation. In: 53rd AIAA/ASME/ASCE/AHS/ASC Structures, Structural Dynamics and Materials Conference. American Institute of Aeronautics and Astronautics; 2012.
38. Barut A, Madenci E, Tessler A. C0-continuous triangular plate element for laminated composite and sandwich plates using the {2,2} – refined Zigzag Theory. *Compos Struct* 2013;106:835–53.
- [39] Iurlaro L, Gherlone M, Di Sciuva M, Tessler A. A multi-scale refined Zigzag Theory for multilayered composite and sandwich plates with improved transverse shear stresses. In: 5th International Conference on Computational Methods for Coupled Problems in Science Engineering. Ibiza, Spain: COUPLED PROBLEMS 2013; 2013.
- [40] Iurlaro L, Gherlone M, Di Sciuva M. A mixed cubic zigzag model for multilayered composite and sandwich plates including transverse normal deformability. In: *Proceedings of the 11th World Conference on Computational Methods*, Barcelona, Spain; 2014. p. 2.
- [41] Iurlaro L, Gherlone M, Di Sciuva M. The (3,2)-mixed refined Zigzag Theory for generally laminated beams: theoretical development and C^0 finite element formulation. *Int J Solids Struct* 2015;73–74:1–19.
- [42] Iurlaro L. Development of Refined Models for Multilayered Composite and Sandwich Structures: Analytical Formulation, FEM Implementation and Experimental assessment. 2015. PhD Thesis, Politecnico di Torino, Italy.
- [43] Tessler A. Refined Zigzag Theory for homogeneous, laminated composite, and sandwich beams derived from Reissner's mixed variational principle. *Meccanica* 2015;50(10):2621–48.
- [44] Reissner E. On a variational theorem in elasticity. *J Math Phys* 1950;29(1–4):90–5.
- [45] Auricchio F, Sacco E. Refined first-order shear deformation theory models for composite laminates. *J Appl Mech* 2003;70(3):381–90.
- [46] Groh RMJ, Weaver PM. On displacement-based and mixed-variational equivalent single layer theories for modelling highly heterogeneous laminated beams. *Int J Solids Struct* 2015;59:147–70.
- [47] Groh RMJ, Weaver PM. A computationally efficient 2D model for inherently equilibrated 3D stress predictions in heterogeneous laminated plates. Part I: model formulation. *Compos Struct* 2016;156:171–85.
- [48] Groh RMJ, Weaver PM. A computationally efficient 2D model for inherently equilibrated 3D stress predictions in heterogeneous laminated plates. Part II: model validation. *Compos Struct* 2016;156:186–217.
- [49] Thurnherr C, Groh RMJ, Ermanni P, Weaver PM. Higher-order beam model for stress predictions in curved beams made from anisotropic materials. *Int J Solids Struct* 2016;97–98:16–28.
- [50] Köppl M, Wagner W. A mixed finite element model with enhanced zigzag kinematics for the non-linear analysis of multilayer plates. *Comput Mech* 2020;65(1):23–40.
- [51] Trinh LC, Groh RMJ, Zucco G, Weaver PM. A strain-displacement mixed formulation based on the modified couple stress theory for the flexural behaviour of laminated beams. *Compos Part B Eng* 2020;185:107740.